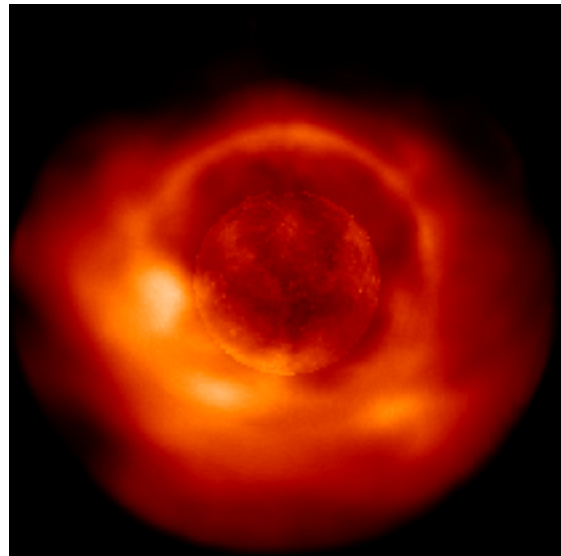


SOHO 7 WORKSHOP:

Coronal Holes and Solar Wind Acceleration

28 September – 1 October 1998

Asticou Inn
Northeast Harbor, Maine



POSTER
ABSTRACT
BOOK

TABLE OF CONTENTS

Abstracts are alphabetized by first author, and poster numbers are given in parentheses before the authors.

(01) Richard C. Altrock	10
<i>A Comparison of Coronal Hole Morphology as Observed with SOHO/EIT and the NSO/SP Coronal Photometer</i>	
(02) Ester Antonucci, Silvio Giordano, and Maria Adele Dodero	10
<i>Velocity distribution of ions and neutral hydrogen in polar coronal holes</i>	
(03) W.I. Axford and J.F. McKenzie	10
<i>Acceleration of the high speed solar wind in coronal holes (Introductory Talk)</i>	
(04) Jean-Loup Bertaux, Erkki Kyrola, Eric Quemerais, Rosine Lallement, Walter Schmidt, Tuula Summanen, Jorge Costa, Teemu Makinen	11
<i>Latitude distribution of solar wind as seen by SWAN in Lyman α and evolution since launch</i>	
(05) R. Betta, S. Orlando, G. Peres and S. Serio	12
<i>On the Stability of siphon flows confined in coronal loops</i>	
(06) R. Bodmer and K. Wilhelm	12
<i>Ne/Mg Ratios Above a Polar Coronal Hole from UV/EUV Observations by SUMER/SOHO</i>	
(07) B. J. I. Bromage, J. R. Clegg, and B. Thompson	12
<i>“Birth” of a large low-latitude coronal hole</i>	
(08) L. F. Burlaga	13
<i>Corotating flows at 1 AU</i>	
(09) Claudio Chiuderi	13
<i>Transition from collisional to collisionless regime in the solar corona</i>	
(10) F. Chiuderi Drago, A. Kerdraon, A. Fludra and E. Landi	13
<i>Radio and UV observations of a Coronal Hole</i>	

(11) J. R. Clegg, P. K. Browning, and B. J. I. Bromage 14
<i>The solar magnetic field as a coronal hole extension forms</i>	
(12) S. R. Cranmer, G. B. Field, and J. L. Kohl 14
<i>The Impact of Ion-Cyclotron Wave Dissipation on Heating and Accelerating the Fast Solar Wind</i>	
(13) I. Cuseri, D. J. Mullan, G. Noci, and G. Poletto 14
<i>Heating and acceleration of the solar wind via gravity damping of Alfvén waves</i>	
(14) R. B. Dahlburg, J. T. Karpen, G. Einaudi, and P. Boncinelli 15
<i>Slow solar wind formation</i>	
(15) Ingolf E. Dammasch 15
<i>Statistical analysis of EUV lines inside/outside coronal hole</i>	
(16) J.M. Davila and L. Ofman 16
<i>Fast solar wind acceleration and heating by nonlinear waves</i>	
(17) G. Del Zanna and B.J.I. Bromage 16
<i>Characterisation of solar coronal holes and plumes using spectroscopic diagnostic techniques applied to SOHO/CDS observations</i>	
(18) D. Dobrzycka, L. Strachan, M.P. Miralles, J.L. Kohl, L.D. Gardner, P. Smith, M. Guhathakurta, and R. Fisher 17
<i>Variation of Polar Coronal Hole properties with Solar Cycle</i>	
(19) D. Dobrzycka, A. Panasyuk, L. Strachan, and J.L. Kohl 17
<i>Comparison of Polar and Equatorial Coronal Holes observed by UVCS/SOHO - Geometry and Physical Properties</i>	
(20) D.A. Falconer, R.L. Moore, J.G. Porter, and D.H. Hathaway 18
<i>Accumulation of Small Coronal Bright Points in the Quiet Magnetic Network</i>	
(21) S. Fineschi, L. Strachan, M. Romoli, J. L. Kohl, G. Noci 18
<i>Electron Density Distribution in Coronal Streamers</i>	

(22) L. A. Fisk	18
<i>Coronal Hole Boundaries and Interactions with Adjacent Regions (Introductory Talk)</i>	
(23) Andrzej Fludra	19
<i>Characteristics of Polar Coronal Holes and their Evolution from EUV Observations</i>	
(24) R. A. Frazin, A. Modigliani, A. Ciaravella, E. Dennis, S. Fineschi, L. D. Gardner, J. Michels, R. O'Neal, J. C. Raymond, G. Noci, and J. L. Kohl	19
<i>UVCS Line Profiles in Coronal Streamers</i>	
(25) A.B. Galvin, F.M. Ipavich, J. Paquette, D. Hovestadt, P. Wurz, and R. Kallenbach	19
<i>SOHO/CELIAS Measurements of Sulfur Isotopes in the Solar Wind</i>	
(26) Sarah Gibson	20
<i>The three-dimensional coronal magnetic field during Whole Sun Month</i>	
(27) Silvio Giordano and Ester Antonucci	20
<i>Fast and Slow Solar Wind Transition at Streamer Borders</i>	
(28) G. Gloeckler, F. M. Ipavich, L. A. Fisk, S. Hefti, T. H. Zurbuchen, and J. Geiss	20
<i>Anomalous isotopic and charge state composition of the solar wind in a CME observed with ACE and Wind.</i>	
(29) Clinton P.T. Groth, Darren L. De Zeeuw, Tamas I. Gombosi, Hal G. Marshall, Kenneth G. Powell, and Quentin F. Stout	21
<i>A Parallel Adaptive 3D MHD Scheme for Modeling Coronal and Solar Wind Plasma Flows</i>	
(30) M. Guhathakurta and E. C. Sittler, Jr.	21
<i>MHD Model of the Large-Scale Corona and the Interplanetary Medium from 1 R_{\odot} to 4 AU using SOHO and Ulysses Observations</i>	
(31) P. Hackenberg, G. Mann, and E. Marsch	22
<i>Plasma Properties in Coronal Funnels</i>	

(32) Viggo H. Hansteen	22
<i>Time dependent heating of the corona and the solar wind</i>	
(33) Karen L. Harvey and Frank Recely	23
<i>Inferring Coronal Hole Boundaries and Their Evolution from He I 1083 nm</i>	
(34) D.M. Hassler, I.E. Dammasch, P. Lemaire, H. Warren, and K. Wilhelm ..	23
<i>Coronal Hole/Streamer Interface Observed with SUMER</i>	
(35) Alan Hood	23
<i>Models of Coronal Plumes</i>	
(36) R.A. Howard	23
<i>Mass Flux in the Solar Wind due to CMEs</i>	
(37) Jude Insley	24
<i>CDS observations of coronal holes</i>	
(38) F.M. Ipavich, G. Gloeckler, T.H. Zurbuchen, S. Hefti, P. Bochsler, L.A. Fisk, R. Kallenbach, J.A. Paquette, R.F. Wimmer-Schweingruber	24
<i>Temporal Behavior of Solar Wind Fe and O in High Speed Stream Onsets</i>	
(39) Harrison P. Jones, Vincenzo Andretta, and Matthew J. Penn	25
<i>He I 1083 nm Asymmetry and EUV Line Shifts in Coronal Holes</i>	
(40) M. Karovska, B. Wood, J. W. Cook, G. E. Brueckner, J. W. Cook	25
<i>Study of Dynamical Properties of Coronal Structures in the Polar Regions</i>	
(41) R. Keppens and J.P. Goedbloed	26
<i>Numerical simulations of stellar winds</i>	
(42) Y.-K. Ko and C. P. T. Groth	26
<i>On the coronal electron temperature profile and coronal heating constrained by in-situ observations</i>	

(43) J. L. Kohl, S. Fineschi, R. Esser, A. Ciaravella, S. R. Cranmer, L. D. Gardner, A. Modigliani, R. Suleiman, and G. Noci	26
<i>UVCS/SOHO Observations of Spectral Line Profiles in Polar Coronal Holes</i>	
(44) M. Kojima, T. Ohmi, A. Yokobe, M. Tokumaru, K. Hakamada	27
<i>The highest solar wind velocity in a polar region estimated from IPS tomography analysis</i>	
(45) P. Lamy, E. Quemerais, M. Bout and A. Llebaria	27
<i>Maps of the Coronal Electron Density from LASCO-C2 Images</i>	
(46) Enrico Landi	27
<i>Observation of transition region fine structures with SUMER and CDS</i>	
(47) Enrico Landi and Massimo Landini	28
<i>Loop models with SOHO observations</i>	
(48) P.Lemaire, K. Bocchialini, V. Aletti, D. Hassler, K. Wilhelm	28
<i>Search for signatures of a coronal hole in transition region lines near disk center</i>	
(49) Xing Li	28
<i>Heating and Cooling of protons in the fast solar wind</i>	
(50) P. C. Liewer, M. Velli and B. E. Goldstein	29
<i>Hybrid Simulations of Wave Propagation and Ion Heating in the Solar Wind using a 1D Expanding Box Model</i>	
(51) Lisa Maccari and the UVCS team	29
<i>Density and Electron Temperature in Coronal Streamers</i>	
(52) Eckart Marsch	30
<i>Solar wind models from the Sun to 1 AU: Constraints by “in situ” and remote sensing measurements (Introductory Talk)</i>	
(53) P.C.H. Martens, K. Tziotziou, and A.G. Hearn	30
<i>Energy and Momentum Deposition in Coronal Holes – Solar Coronal Hole Simulations Compared with Interpretations of Yohkoh-SXT and SOHO-UVCS Observations</i>	

(54) D. J. Michels, M. J. Koomen, S. P. Plunkett, S. Paswaters, S. T. Wu, and A.-W. Wang	31
<i>Source of the Equatorial Plasma Sheet at Solar Minimum</i>	
(55) Mari Paz Miralles, Leonard Strachan, Larry D. Gardner, Peter L. Smith, John L. Kohl, Madhulika Guhathakurta, and Richard R. Fisher	31
<i>Physical Properties of Coronal Hole/Streamer boundaries, and adjacent regions as observed by Spartan 201</i>	
(56) R. L. Moore, D. A. Falconer, J. G. Porter, S. T. Suess	32
<i>Coronal Heating by Magnetic Explosions</i>	
(57) L. Ofman, M. Romoli, G. Poletto, G. Noci, J. L. Kohl, R. A. Howard, C. St.Cyr, C. DeForest	32
<i>SOHO Observations of Density Fluctuations in the Solar Wind</i>	
(58) E. L. Olsen and E. Leer	33
<i>A study of solar wind acceleration based on the gyro-tropic transport equations</i>	
(59) Hari Om Vats, M.R. Deshpande, M. Mehta, K.J. Shah and C.R. Shah	33
<i>Study of coronal rotation by solar radio flux measurements</i>	
(60) Spiros Patsourakos	34
<i>Determination of the Flux of matter in a polar coronal hole via coordinated observations between SOHO/SUMER and ground during the 1998 total eclipse</i>	
(61) Yu. V. Pisanko	34
<i>MHD Modeling of the Polar Solar Wind Acceleration</i>	
(62) S. Poedts, A. Rogava, and S.M. Mahajan	34
<i>Velocity shear induced effects in the solar wind</i>	
(63) A. I. Poland and J. Chae	35
<i>Energetics of the Lower Transition Region</i>	
(64) J. G. Porter, D. A. Falconer, and R. L. Moore	36
<i>Microflares and the Heating of Plumes Over Enhanced Network</i>	

(65) John C. Raymond	36
<i>Composition and Elemental Abundance Variations in the Solar Corona Solar Atmosphere and Solar Wind (Introductory Talk)</i>	
(66) Eugene Romashets	36
<i>Velocity of Toroidal Magnetic Clouds From the Sun to the Earth's Orbit</i>	
(67) M. Romoli, et al.	37
<i>Electron Densities measured with UVCS/WLC</i>	
(68) U. Schuehle, W. Curdt, S. Solanki, K. Stucki, and K. Wilhelm	37
<i>Signatures of coronal hole spectra between 700 and 1500 Angstrom measured with SUMER on SOHO</i>	
(69) R. Schwenn, B. Inhester, B. Podlipnik, N. Srivastava, G. Stenborg	37
<i>The rotation of the solar corona - an analysis of LASCO Fe XIV emission data during solar minimum activity</i>	
(70) Gregory Slater	38
<i>Seven Years of Coronal Hole Observations With the SXT</i>	
(71) P. L. Smith, R. Suleiman, L. D. Gardner, M. Cosmo, N. Atkins, and J. L. Kohl	38
<i>"Flat Fields" for UVCS Detectors</i>	
(72) J. Solomon, F. Pierre, N. Cornilleau-Wehrin, P. Canu, E. E. Scime, A. Balogh, R. Forsyth	38
<i>On the electron heat flux regulation in the solar wind through wave-particle interactions</i>	
(73) D. Spadaro, R. Ventura, M. Alicata, S. Fineschi, C. Benna, A. Ciaravella, R. O'Neal, A. Modigliani, R. Suleiman, G. Noci, and J. L. Kohl	39
<i>A study of the coronal hole - streamer interface</i>	
(74) N. Srivastava, R. Schwenn, B. Inhester, G. Stenborg and B. Podlipnik ...	39
<i>Acceleration Profile Of the Slow Solar Wind as inferred from gradual mass ejections observed by LASCO</i>	

(75) G. Stenborg, Rainer Schwenn, N. Srivastava, B. Inhester, B. Podlipnik, M. Rovira, and C. Francile	39
<i>Recent observations of the solar corona with a new ground-based mirror coronagraph in Argentina (MICA)</i>	
(76) L. Strachan, Y-K. Ko, A.V. Panasyuk, D. Dobrzycka, J.L. Kohl, M. Romoli, G. Noci, S.E. Gibson, D.A. Biesecker	40
<i>Constraints on Coronal Outflow Velocities derived from UVCS Doppler Dimming Measurements and In-Situ Charge State Data</i>	
(77) K. Stucki, S.K. Solanki, I. Ruedi, J.O. Stenflo, A. Brkovic, U. Schuehle, K. Wilhelm, and M.C.E. Huber	40
<i>Coronal Holes versus normal Quiet Sun observed with SUMER</i>	
(78) S. T. Suess, A.-H. Wang, S. T. Wu, S. F. Nerney	41
<i>Streamer evaporation</i>	
(79) S. Suess, G. Poletto, G. Simnett	41
<i>Ulysses-UVCS Coordinated Observations.</i>	
(80) R. M. Suleiman, J. L. Kohl, R. Frazin, A. Ciaravella, S. R. Cranmer, L. D. Gardner, R. Hauck, A. V. Panasyuk, P. L. Smith and G. Noci	42
<i>UVCS/SOHO Observations of H I Lyman Alpha Line Profiles in Coronal Holes at Heliocentric Heights above 3.0 R_⊙</i>	
(81) C.-Y. Tu, E. Marsch, K. Wilhelm, W. Curdt	42
<i>Ion temperatures as observed in the solar corona and obtained in a solar wind model</i>	
(82) A. M. Vasquez, J. C. Raymond, and A. Van Ballegooijen	43
<i>UVCS observations of coronal streamers and theoretical models: structure and oxygen abundance</i>	
(83) M. Velli, P.C. Liewer and D. Kondrashov	43
<i>Alfvén Waves from the Transition Region and “Solar Tornadoes”</i>	
(84) Peter Young	43
<i>CDS/SOHO spectral variations in and around coronal holes</i>	

(85) L. Zangrilli, P. Nicolosi, G. Poletto 44

Latitudinal properties of the Lyman alpha and O VI profiles in the extended solar corona

(86) X.P. Zhao and J.T. Hoeksema44

Radial variation of the coronal helmet streamer belt

(87) F. Zuccarello 44

Elemental abundances in different solar regions

(88) T. H. Zurbuchen, S. Hefti, L. A. Fisk, G. Gloeckler, N. A. Schwadron, R. von Steiger 45

The Transition from Fast and Slow Solar Wind: Experimental Constraints on Solar Wind Theories

LATE ABSTRACTS:

(89) A. Ciaravella, J. Raymond, B. Thompson, J. Li, R. O’Neal, J. Kohl, and G. Noci 45

Physical and Dynamical Parameters of a CME observed with SOHO

(90) A. H. Gabriel, F. Bely-Dubau, C. David, P.Lamy and E. Quemerais 46

Enhanced abundance of oxygen and iron in polar coronal holes, from CDS, SUMER and LASCO data

(01)

A Comparison of Coronal Hole Morphology as Observed with SOHO/EIT and the NSO/SP Coronal Photometer

RICHARD C. ALTROCK (AIR FORCE RESEARCH LAB., SUNSPOT, NM 88349)

Solar coronal holes are easily seen in images produced by the Extreme Ultraviolet Imaging Telescope on the SOHO mission. The best contrast appears to be in Fe XII 19.5 nm. Coronal holes are also seen in “full-disk” maps produced from observations of Fe XIV 530.3 nm obtained with the coronal photometer at the National Solar Observatory at Sacramento Peak. The photometer is fed by the 40-cm coronagraph of the John W. Evans Solar Facility. Such observations have been obtained daily, whenever possible, since 1975. These maps are produced by concatenating 14 days (or fewer, if interpolation must be used) of scans of the corona made at 1.15 solar radii and projecting them onto a sphere. Thus, an assumption is made of no evolution in the morphology of coronal holes over a two-week period. Rigid solar rotation at the Carrington rate is also assumed. This paper will compare the morphology of coronal holes as observed in the two lines on days selected from the entire EIT database. This will test the assumption of stationarity and rigid rotation of the corona as well as the issue of whether ground-based observations might be used as a proxy to extend the coronal hole data obtained by EIT to periods before and after the SOHO epoch.

This paper is supported by the Air Force Office of Scientific Research. Data reduction and graphics programming was done by Timothy W. Henry.

(02)

Velocity distribution of ions and neutral hydrogen in polar coronal holes

ESTER ANTONUCCI (OSSERVATORIO ASTRONOMICCO DI TORINO, 10025 PINO TORINESE, ITALY), AND SILVIO GIORDANO, MARIA ADELE DODERO (DIPARTIMENTO DI FISICA GENERALE, UNIVERSITY OF TORINO, 10125 TORINO, ITALY)

A remarkable characteristic of the polar coronal hole regions, and in general of the regions of open magnetic field lines outside streamers, is that the profiles of the ultraviolet spectral lines are much broader than in the streamer belt and that the effect is enhanced for lines emitted by heavier elements. By combining measurements of line broadenings with those relative to Doppler dimming of line intensity, it is possible to infer both the velocity of expansion of the solar corona in polar regions and an upper limit for the width of the velocity distribution of ions and neutral hydrogen in radial direction. Here we present the results obtained with UVCS between 1.5 and 2.4 solar radii for the outflow velocity and velocity distributions along the radial on April 6–9, 1996. In the analysis we use the new calculations of the O VI 1037, 1032 Doppler dimming functions obtained by Doderò, Antonucci and Martin 1998.

(03)

Acceleration of the high speed solar wind in coronal holes

W. I. AXFORD AND J. F. MCKENZIE (MPAE, KATLENBURG-LINDAU, GERMANY)

The high speed solar wind is long-lasting and relatively steady in its characteristics. It is associated with coronal holes and unipolar magnetic fields. The energy, mass and magnetic field fluxes are constants of the motion in this case and may be determined at any distance

from the Sun. As a consequence, there is little in the way of free parameters to be chosen and indeed we find that, given a realistic magnetic field geometry and constraining the plasma density at the base of the corona to be about 10^8 /cm³, one is forced to a solution in which the plasma is heated strongly close to the Sun. It reaches temperatures of the order of 5-10 million degrees per amu and accelerates rapidly with the sonic point being at about $2 R_s$.

Observations of the proton temperature/pressure distributions by the Helios spacecraft, of the preferred heating and acceleration of heavy species, and of the rapid heating required, suggest that the heating is in some way associated with cyclotron absorption of waves emitted directly from the coronal base, i.e. from the chromospheric network. The precise nature of the waves and the dissipation process involved is not understood at present although, by elimination, we deduce that the source should lie in small-scale, flare-like events occurring in the network. Cyclotron absorption can lead to large temperature anisotropies in the the corona which, in the case of protons, should be quenched by plasma instabilities but, in the case of minor species, can persist since they do not contribute significantly to the overall pressure anisotropy.

The characteristics of the chromospheric network underlying coronal holes and the neighbouring quiet coronal regions are indistinguishable. Furthermore the energy fluxes in the form of high speed solar wind, in the case of coronal holes, and radiation from the transition region and elsewhere, in the case of the magnetically-closed corona, are about the same. It is therefore reasonable to argue that the heating mechanisms should also be the same in each case, namely high-frequency Alfvén waves emitted from the network. The alternative suggestion that the quiet, closed-field corona is heated by the dissipation of twisted, force-free magnetic fields as nano-flares does not appear to be viable since the low- frequency Alfvén waves that lead to the necessary twisting of the field in closed regions should be easily detected as out-going waves in the high speed solar wind; these are not present with anything like the energy flux required.

On extending these ideas to include phenomena occurring in the network itself we find that it is unlikely that there should be a significant FIP effect in the high speed wind, apart from the special case of helium, and that the charge states of ions in the wind is probably determined by a high energy tail of the electron distribution since the electron temperatures expected are otherwise too low to be effective.

(04)

Latitude distribution of solar wind as seen by SWAN in Lyman α and evolution since launch

JEAN-LOUP BERTAUX (1), ERKKI KYROLA (2), ERIC QUEMERAIS (1), ROSINE LALLEMENT (1), WALTER SCHMIDT (2), TUULA SUMMANEN (2), JORGE COSTA (1), AND TEEMU MAKINEN (2)

(1) SERVICE D'AÉRONOMIE DU CNRS, BP. 3, 91371 VERRIÈRES-LE-BUISSON, FRANCE

(2) FINNISH METEOROLOGICAL INSTITUTE, P.O. BOX 503, FI 00101 – HELSINKI, FINLAND

SWAN is the first space instrument dedicated to the monitoring of the latitude distribution of the solar wind by the Lyman alpha method. The distribution of interstellar H atoms in the solar system is carved by their destruction during ionization charge-exchange with solar wind protons. Maps of sky L-alpha emissions were recorded regularly since launch. The region of maximum emission, located in the upwind hemisphere, deviates strongly from the pattern that could be expected from a solar wind constant with latitude. It is divided in two lobes by a depression aligned with the solar equatorial plane called the Lyman alpha groove already noted in 1976 Prognoz data. The North lobe is much brighter than the South lobe. These two characteristics can be explained qualitatively by an enhanced ionization along the neutral sheet where is concentrated the slow solar wind, which results from the higher solar wind mass flux. The groove is the direct imprint on the sky of the enhanced carving by the slow solar wind,

at this time of solar minimum, when the tilt angle of the neutral sheet is small. Comparisons of maps at two years interval show that the groove is filling with the ascending phase of the solar cycle, a sign of decreasing anisotropy most likely linked to the increasing inclination of the neutral sheet. A quantitative analysis of the solar wind distribution will also be presented, yielding a clear dichotomy between the fast solar wind and the slow solar wind.

(05)

On the Stability of siphon flows confined in coronal loops

R. BETTA, S. ORLANDO, G. PERES AND S. SERIO

We use a time-dependent hydrodynamic model to study the dynamics of siphon flows triggered by differences of pressure or heat deposition in the two footpoints of a coronal loop.

We show that pressure driven stationary flows in an uniformly heated loop are generally not stable, whereas those driven by asymmetries in the heating function may be stable. We also show that, in these cases, relatively cool loops might be filled far above their static pressure scale height.

(06)

Ne/Mg Ratios Above a Polar Coronal Hole from UV/EUV Observations by SUMER/SOHO

R. BODMER AND K. WILHELM (MAX-PLANCK-INSTITUT FÜR AERONOMIE, KATLENBURG-LINDAU, GERMANY)

The enrichment of elements with low first ionization potential (FIP) in the solar corona and solar wind with respect to photospheric abundances is an important source of information about the origin of the solar wind. While the solar wind composition can be probed in situ by mass spectrometers, the composition in its source region is reflected in UV and EUV emission lines. We use observations of the northern polar coronal hole during the SOHO roll manoeuvre on September 3, 1997, where the SUMER slit was oriented in east-west direction, so that polar plumes and inter-plume lanes could be observed simultaneously. Electron densities (from Si VIII or Mg VIII) and temperatures (from Mg IX) have been deduced from line radiance ratios. Line intensity ratios of Ne VIII (high FIP) and Mg VIII (low FIP) from bright polar plumes and dark inter-plume lanes reveal strong abundance variations within the polar coronal hole. The comparison with photospheric abundances yields a FIP fractionation within inter-plume lanes, but a much stronger effect is observed in plumes. Comparing these findings to ULYSSES observations of high speed solar wind from polar coronal holes, where the abundances are fairly constant and show almost no FIP fractionation, we conclude that the plumes do not substantially contribute to the solar wind. More detailed work is needed to figure out, whether the abundances in inter-plume lanes are consistent with the solar wind, or, if the observed residual fractionation comes from contamination by faint plumes along the line of sight.

(07)

“Birth” of a large low-latitude coronal hole

B. J. I. BROMAGE, J. R. CLEGG, AND B. THOMPSON

The August 1996 “Elephant’s Trunk coronal hole” began to develop in June from an interaction between the extended structure of a large active region located just south of the equator and

the magnetic arcade structure of the north polar crown. Its evolution is followed using SOHO EUV images and magnetic field modelling of solar magnetogram data.

(08)

Corotating flows at 1 AU

L. F. BURLAGA (LABORATORY FOR EXTRATERRESTRIAL PHYSICS, NASA GODDARD SPACE FLIGHT CENTER, CODE 692, GREENBELT, MARYLAND 20771)

Corotating flows at 1 AU typically have low densities high temperatures and high speeds. A corotating stream is bounded in front by a thin stream interface across which the density decreases the temperature and speed increase, the flow direction changes and the magnetic field strength approaches a local maximum. Corotating streams have a broad range of sizes, passing a spacecraft in an interval lasting from several hours to several days. Some corotating streams recur for several solar rotations, others evolve significantly from one solar rotation to the next, and still others appear on one solar rotation but not on the previous or following rotations. The speeds in corotating streams may be greater than 700 km in some cases as small as a few hundred km/sec. Previous results showed that corotating streams near Earth may originate from equatorial extensions of polar coronal holes and from small near-equatorial coronal holes. Problems concerning corotating streams that might be solved with SOHO observations include the nature of corotating streams associated with near-equatorial coronal holes, the properties of transient corotating streams, and the significance of slow corotating 'streams'.

(09)

Transition from collisional to collisionless regime in the solar corona

CLAUDIO CHIUDERI (DEPT. OF ASTRONOMY, UNIVERSITY OF FLORENCE, LARGO E. FERMI, 5 - 50125 FIRENZE, ITALY)

The transition from collisional to collisionless regime is studied by the means of a numerical codes that solves the Fokker-Planck equation in (1D + 2V) phase space. The velocity space is assumed to have cylindrical geometry. The code allows a first investigation of the efficiency of the process of velocity filtration.

(10)

Radio and UV observations of a Coronal Hole

F. CHIUDERI DRAGO, A. KERDRAON, A. FLUDRA AND E. LANDI

An equatorial Coronal Hole was clearly observed around the central meridian transit on October 19, 1996 by the the EIT and CDS instruments onboard SOHO and by the Radioheliograph of Nancay (France) at 164, 236, 327 and 408 MHz. A comparison between UV and radio observations can supply important information on the Coronal Hole structure in the Transition Region and low Corona.

(11)

The solar magnetic field as a coronal hole extension forms

J. R. CLEGG, P. K. BROWNING, AND B. J. I. BROMAGE

An analytical solution is presented to the linear force-free field problem within a spherical shell, representing the solar corona. The inner boundary conditions are obtained using a novel technique, whilst the sensitivity of solutions to modelled outer boundary conditions and to an assumed “global” magnetic helicity is tested. The results provide insight into both visible and far solar surface magnetic fields during the coronal hole extension event of August 1996. A sufficient representation of the background magnetic field is seen as a precursor to the development of numerical modelling of local coronal hole regions.

(12)

The Impact of Ion-Cyclotron Wave Dissipation on Heating and Accelerating the Fast Solar Wind

S. R. CRANMER, G. B. FIELD, AND J. L. KOHL (SAO)

We present theoretical models of the acceleration and heating of major and minor ions in the fast solar wind. We examine the compatibility between these models and spectroscopic determinations of velocity distribution functions from the SOHO Ultraviolet Coronagraph Spectrometer (UVCS/SOHO). It has become clear that to understand the dominant physical mechanisms in the nearly collisionless solar corona, each particle species must be treated individually, with its own anisotropic velocity distribution. Even minor ions which do not affect the overall energy and momentum budget of the plasma are important to measure as constraints on different theories.

The primary momentum and energy deposition mechanism we investigate is the dissipation of high-frequency (ion-cyclotron resonant) Alfvén waves, which can accelerate and heat ions differently depending on their charge and mass. Because the origin of these still-unobserved (kilohertz frequency) waves has not yet been determined, we model the waves as either propagating up from the coronal base or generated in the wind via turbulent cascade; we discuss methods of distinguishing between these two scenarios using the spectroscopic data.

The models which best reproduce the SOHO and in-situ measurements can strongly constrain the physical processes behind the acceleration and heating of the solar wind. Also, they are useful as predictors of many qualitative features of the power spectrum of waves in the corona. Indeed, the more ionic species that are observed spectroscopically, the greater the extent in frequency space the wave spectrum can be inferred.

This work is supported by the National Aeronautics and Space Administration under grant NAG5-3192 to the Smithsonian Astrophysical Observatory, by Agenzia Spaziale Italiana, and by Swiss funding agencies.

(13)

Heating and acceleration of the solar wind via gravity damping of Alfvén waves

IOLANDA CUSERI (DIPARTIMENTO DI ASTRONOMIA E SCIENZA DELLO SPAZIO, C/O OSSERVATORIO ASTROFISICO DI ARCETRI, LARGO E. FERMI N. 5, 50125 FLORENCE, ITALY)

We present here two-fluid models for the heating of the solar corona and acceleration of the solar wind, based on the dissipation of Alfvén waves by gravity damping. This mechanism was proposed by Khabibrakhmanov and Mullan (1994) but, so far, has not been applied in modeling efforts. Khabibrakhmanov and Mullan theory has been extended to give an expression for the evolution of the Alfvén wave amplitude as a function of the local parameters of the atmosphere. The system of equations which we use includes, in the proton energy equation, a gravity dissipation term, and, in the momentum equation, a different wave acceleration term than usually adopted. Initial conditions for the integration of the equations are compatible with recent Ulysses measurements and the integration proceeds from 1 AU towards the base of the solar corona. Our results show that the gravity damping of Alfvén waves heats the solar plasma to coronal values and accelerates the solar wind to 600-700 km/s. Model predictions at low heliocentric distances compare favorably with recently acquired UVCS data.

(14)

Slow solar wind formation

R. B. DAHLBURG AND J. T. KARPEN (NAVAL RESEARCH LABORATORY, WASHINGTON, DC USA), G. EINAUDI (UNIVERSITY OF PISA, PISA, ITALY), AND P. BONCINELLI (UNIVERSITY OF FLORENCE, FLORENCE, ITALY)

Recent work on a magnetohydrodynamic mechanism which accounts for several fundamental properties of the slow solar wind, in particular its variability, latitudinal extent, and bulk acceleration is reviewed. In view of the well-established association between the streamer belt and the slow wind, our model begins with a simplified representation of a section of a streamer beyond the underlying coronal helmet, consisting of a neutral sheet embedded in a plane fluid wake. This wake—neutral sheet configuration is characterized by two parameters which vary with distance from the Sun: the ratio of the cross-stream velocity scale to the neutral sheet width, and the ratio of the typical Alfvén velocity to the typical flow speed far from the neutral sheet. Depending on the value of these parameters, linear theory predicts that three kinds of instabilities can develop when this system is perturbed: a resistive instability, and two ideal fluid instabilities with different cross-stream symmetries (varicose and sinuous).

In the innermost, magnetically dominated region beyond the helmet cusp, the streamer is resistively and ideally unstable, evolving from tearing-type reconnection in the linear regime to a nonlinear, varicose fluid instability which forms travelling magnetic islands similar to features recently revealed by the large-angle spectroscopic coronagraph (LASCO) on the joint ESA/NASA Solar and Heliospheric Observatory (SOHO). During this process, the center of the wake is accelerated outward and the cross-stream velocity profile broadens slightly. Past the Alfvén point, where the kinetic energy exceeds the magnetic energy, the resistive mode is suppressed but an ideal, sinuous, fluid mode can develop, producing additional acceleration up to typical slow wind speeds. Further from the Sun, the system becomes highly turbulent due to the development of ideal secondary instabilities, thus halting the acceleration and producing strong radially-directed filamentation throughout the core of the wake. The implications of this model for the origin and evolution of the slow solar wind are discussed, and the predicted properties are compared with current observations from SOHO.

(15)

Statistical analysis of EUV lines inside/outside coronal hole

INGOLF E. DAMMASCH (MAX-PLANCK-INSTITUT FUER AERONOMIE, D-37191 KATLENBURG-LINDAU, GERMANY)

Two SUMER studies of September 1996 will be presented. Spatial scans, long exposure times and a broad spectral window provide reliable average line profiles for separate locations (corona, coronal hole, quiet Sun, bright and dark regions on disk) and for different temperatures (Carbon IV, Neon VIII). Relative intensities and their distributions, line positions and line widths will be presented and compared to results of SUMER full disk scans taken in February 1996.

(16)

Fast solar wind acceleration and heating by nonlinear waves

J.M. DAVILA (NASA GSFC, CODE 682, GREENBELT, MD 20771)

L. OFMAN (RAYTHEON STX/NASA GSFC, CODE 682, GREENBELT, MD 20771)

New SOHO observations indicate that waves are present in the coronal holes. These waves are detected directly as brightness fluctuations in plumes by EIT and the UVCS instruments, and indirectly by line broadening of Ly-alpha and minor ion emission lines. To model the fast solar wind acceleration by nonlinear waves we solve the self-consistent time-dependent, nonlinear, resistive 2.5-D MHD equations driven by Alfvén waves. We find that when sufficient flux of Alfvén wave is present large amplitude nonlinear solitary-like waves are generated in the model coronal hole. The solar wind speed and the amplitude of the velocity fluctuations increases with the amplitude of the magnetic field and the driving Alfvén waves at the base of the corona. The required Alfvén wave flux is consistent with the observed wave signatures in coronal hole. In addition to the acceleration these waves contribute to heating by dissipating in small scale structures, such as plumes. We investigate the self-consistent contribution to heating due to the nonlinear waves.

(17)

Characterisation of solar coronal holes and plumes using spectroscopic diagnostic techniques applied to SOHO/CDS observations

G. DEL ZANNA AND B. J. I. BROMAGE (UNIVERSITY OF CENTRAL LANCASHIRE PRESTON PR1 2HE UK)

Results from a series of SOHO/Coronal Diagnostic Spectrometer (CDS) observations of coronal holes and plumes are presented, including analysis of a low-latitude plume, observed in August 1996. Spectroscopic diagnostic techniques using the CHIANTI atomic database are applied to derive the plasma parameters: electron density; temperature; element abundances; and filling factors. The methods employed are mainly based on line intensity ratios and differential emission measure analysis. The results are compared with quiet sun values. Coronal electron densities in the holes are found to be about $2 \times 10^8 \text{ cm}^{-3}$, a factor of two-three lower than in the quiet sun. The plasma thermal distribution exhibits differences between coronal holes, the quiet sun and plumes. For example, the peak of the emission in coronal holes is at a lower temperature (about 800000 K) than in the quiet sun (about a million degrees), while plumes show a different distribution, closer to an isothermal state. Differences in the element abundances of the various features are also presented and discussed.

(18)

Variation of Polar Coronal Hole properties with Solar Cycle

D. DOBRZYCKA, L. STRACHAN, M. P. MIRALLES, J. L. KOHL, L. D. GARDNER, P. SMITH
(CENTER FOR ASTROPHYSICS, CAMBRIDGE, MA 02138)

AND M. GUHATHAKURTA, & R. FISHER (NASA/GSFC, GREENBELT, MD 20771)

H I Lyman alpha observations of polar coronal holes were obtained from three SPARTAN-201 flights (in 1993, 1994, and 1995) and the more recent UVCS/SOHO mission. These data span several years of the declining phase, the minimum, and currently rising phase of a solar cycle. We apply the latest laboratory calibration to the UVCS/SPARTAN data and analyze them using various diagnostic techniques. We obtain constraints on the changes of the H I Lyman alpha intensity, profile, hydrogen line-of-sight velocity distribution and outflow velocities. We compare UVCS/SPARTAN H I Lyman alpha observations with UVCS/SOHO to characterize variation of the plasma parameters in the polar coronal holes over a five year period.

This work is supported by NASA under Grant NAG 5-613 to the Smithsonian Astrophysical Observatory and by NASA under Grant NAG5-3192 to the Smithsonian Astrophysical Observatory, by the Italian Space Agency, and by Swiss Funding Agencies.

(19)

Comparison of Polar and Equatorial Coronal Holes observed by UVCS/SOHO – Geometry and Physical Properties

D. DOBRZYCKA, A. PANASYUK, L. STRACHAN, J. L. KOHL (CENTER FOR ASTROPHYSICS, CAMBRIDGE, MA 02138)

We present our analysis of the UVCS/SOHO data acquired during the period of the Whole Sun Month campaign (August 10 - September 08, 1996) when the Sun was near the minimum of solar activity. At that time the north and south polar coronal holes were large, stable structures and at the end of August 1996 a large trans-equatorial coronal hole appeared on the east limb. UVCS/SOHO obtained H I Lyman alpha and O VI (103.2,103.7 nm) observations of the polar coronal holes and the equatorial coronal hole as it was crossing the east solar limb in late August 1996 and then, the west limb in September 1996.

We compare the H I Lyman alpha and O VI (103.2,103.7 nm) intensities, line-of-sight velocity distributions, and kinetic temperatures for hydrogen and O^{5+} ions in both types of coronal holes. Detailed analysis of the emission line intensities, as well as the line width distribution allowed us to put constraints on the geometry of the boundaries of the coronal holes. We modeled the boundaries with flow tubes that expand radially or super-radially and found evidence for superradially diverging geometry for both polar and equatorial coronal holes. Measurements of the O VI (103.2 nm) to O VI (103.7 nm) line ratio indicate that the equatorial coronal hole may have O^{5+} outflow velocities that are lower than those from polar coronal holes.

This work was supported by NASA under Grant NAG5-3192 to the Smithsonian Astrophysical Observatory, by the Italian Space Agency, and by Swiss Funding Agencies.

(20)

Accumulation of Small Coronal Bright Points in the Quiet Magnetic Network

D. A. FALCONER, R. L. MOORE, J. G. PORTER, AND D. H. HATHAWAY

We have extended our examination of the magnetic origin of coronal heating in quiet regions by analyzing a time series of SOHO/EIT coronal images aligned with a Kitt Peak magnetogram. Previously (Falconer et al. 1998, "Network Coronal Bright Points: Coronal Heating Concentrations Found in the Solar Magnetic Network," ApJ, 501, in press) we spatially filtered single images and superimposed them on Kitt Peak magnetograms. This showed a coronal network that traces and stems from the magnetic network and that includes bright points that have a significant coincidence with network neutral lines. From the time series of coronal images, we find that different parts of the magnetic network brighten as network bright points at different times, that smaller network bright points have shorter lives, and that over a span of several hours much more of the magnetic network is covered by the accumulated bright points than in a single coronal image. These results strengthen the view that this low-lying activity in the magnetic network, via the generation of MHD waves, is the main source of the extended heating that powers the entire quiet corona and drives the solar wind.

(21)

Electron Density Distribution in Coronal Streamers

S. FINESCHI, L. STRACHAN, M. ROMOLI, J. L. KOHL, AND G. NOCI

The electron distribution along the line of sight (los) in coronal streamers is derived from UVCS observation of the Hydrogen Lyman series lines. The resonant scattered component of these lines is proportional to the electron density integrated along the los ($\langle n_e \rangle$). The collisional component, on the other hand, is proportional to $\langle n_e^2 \rangle$. The ratio between the resonant to the collisional components ($\langle n_e \rangle^2 / \langle n_e^2 \rangle$) is used to derive the level of inhomogeneity in the electron density (filling factor).

This analysis is applied to streamer structures observed during the minimum of the solar cycle.

(22)

Coronal Hole Boundaries and Interactions with Adjacent Regions

L. A. FISK (UNIVERSITY OF MICHIGAN)

Understanding coronal hole boundaries present interesting challenges: they exhibit rotational properties distinct from the underlying photosphere; they have a particular evolution throughout the solar cycle; they can be the site of the release of Coronal Mass Ejections and other dynamic phenomena. A review will be presented of some of the recent observations and theoretical concepts for the behavior of coronal hole boundaries and their interactions with the adjacent corona. Some emphasis will be placed on the information that is available in observations of the plasma, compositional, and magnetic field properties of the solar wind for revealing coronal dynamics and structures.

(23)

Characteristics of Polar Coronal Holes and their Evolution from EUV Observations

ANDRZEJ FLUDRA (RUTHERFORD APPLETON LABORATORY, UK; NASA GSFC, CODE 682.3, GREENBELT, MD 20771, USA)

Regular weekly observations of the North and South polar coronal holes in 20 EUV lines have been carried out with the Coronal Diagnostic Spectrometer (CDS) since September 1997. Electron densities of the coronal hole and plumes are derived from the density-sensitive lines of Si IX and Si X, up to 1.15 solar radii above the limb. The electron temperature from line ratios, a differential emission measure, and the relative Neon/Magnesium abundance are calculated for the coronal hole and plumes. Evolution of the coronal hole characteristics is discussed, aided by the daily CDS synoptic images in He I, O V, and Mg IX lines.

(24)

UVCS Line Profiles in Coronal Streamers

R. A. FRAZIN ¹, A. MODIGLIANI ², A. CIARAVELLA ¹, E. DENNIS ¹, S. FINESCHI ², L. D. GARDNER ¹, J. MICHELS ¹, R. O'NEIL ¹, J. C. RAYMOND ¹, G. NOCI ², AND J. L. KOHL ¹

¹ SMITHSONIAN ASTROPHYSICAL OBSERVATORY, 60 GARDEN ST., CAMBRIDGE, MA 02138

² UNIVERSITÀ DI FIRENZE, I-50125, ITALY

We used the Ultraviolet Coronagraph Spectrometer (UVCS) on the Solar and Heliospheric Observatory (SoHO) to obtain line profiles of several ions in coronal streamers between 1.3 R_{\odot} and 4 R_{\odot} . We discuss constraints on slow wind acceleration mechanisms implied by the line widths. This work is supported by the National Aeronautics and Space Administration under grant NAG-3192 to the Smithsonian Astrophysical Observatory.

(25)

SOHO/CELIAS Measurements of Sulfur Isotopes in the Solar Wind

A.B. GALVIN, F.M. IPAVICH, J. PAQUETTE, D. HOVESTADT, P. WURZ, AND R. KALLENBACH

We present the first measurements of sulfur isotope ratios (Sulfur-32, Sulfur-33, Sulfur-34) in the solar wind using data from the Charge, Element, Isotope Analysis System (CELIAS) experiment on the SOHO spacecraft. The CELIAS Mass Time-of-Flight (MTOF) sensor is a high resolution mass spectrometer designed to make both elemental and isotopic observations of the solar wind. The CELIAS Proton Monitor (PM) provides simultaneous information on solar wind conditions (speed, density, thermal velocity). We present observations from different time periods. Our sulfur results to date indicate solar wind sulfur isotope ratios similar to meteoritic values.

(26)

The three-dimensional coronal magnetic field during Whole Sun Month

SARAH GIBSON (CATHOLIC UNIVERSITY OF AMERICA/NASA GSFC CODE 682, NASA/GSFC, GREENBELT, MD, 20771)

Using a variety of models and observations of the photospheric magnetic field as a boundary condition, we find a three-dimensional coronal magnetic field which qualitatively matches many of the coronal features observed by coronagraphs and imaging telescopes during the Whole Sun Month (WSM) campaign (August 10 - September 8, 1996). Moreover, regions of open field at the solar surface can be directly linked to high speed solar wind observed by the WIND satellite: specifically, we find that the sources of the two fastest wind streams appear to correspond to the two regions that have been the main foci of the WSM analysis: the equatorial extension of the north coronal hole (known as the Elephant's trunk), and the azimuthally invariant streamer belt region on the opposite side of the sun. Furthermore, we quantitatively compare the different model predictions of coronal plasma and solar wind properties to observations for the streamer belt region, and consider the implications this comparison has for the various model assumptions.

(27)

Fast and Slow Solar Wind Transition at Streamer Borders

SILVIO GIORDANO AND ESTER ANTONUCCI

We present an analysis of the transition layer between fast and slow solar wind which is running along the borders of the streamer observed on June 4 1996 with the Ultraviolet Coronagraph Spectrometer (UVCS) on the Solar Heliospheric Observatory (SOHO). The analysis is performed according to the OVI ratio diagnostics. This equatorial streamer is particularly interesting for its simple configuration. In the inner part of the streamer, where the plasma is confined in closed magnetic field lines, the velocity distributions of the oxygen ions and the neutral hydrogen are predominantly thermal. The non-thermal component of the ion and neutral hydrogen velocity, which is negligible in the inner part of the streamer, is increasing slowly with height along the streamer axis and abruptly across the streamer border, in correspondence to the transition between slow and fast solar wind.

(28)

Anomalous isotopic and charge state composition of the solar wind in a CME observed with ACE and Wind.

G. GLOECKLER, F. M. IPAVICH, L. A. FISK, S. HEFTI, T. H. ZURBUCHEN, AND J. GEISS

The isotopic and charge state composition of the solar wind observed with the Solar Wind Ion Composition Spectrometer (SWICS) and the Solar Wind Ion Mass Spectrometer (SWIMS) spectrometers on ACE in the 2-3 May, 1998 CME was highly unusual, showing to the best of our knowledge, the largest deviations from the typical solar wind composition. Here we report only our preliminary observations of solar wind hydrogen, helium and several heavy ion species (e.g., C, N, Mg, and Si) using data from the ACE as well as the Wind spacecraft composition instruments. With SWICS we can determine both the mass and charge of a solar wind ion and thus separate He^+ from solar wind heavy ions with mass/charge of 4. In addition, because we measure the ion velocity distribution, we easily separate solar wind from pickup He^+ . We find

that the $\text{He}^+/\text{He}^{++}$ density ratio is variable, reaching values as high as 2.5. $^3\text{He}^{++}$ is also well identified with SWICS. The solar wind $^3\text{He}^{++}/^4\text{He}^{++}$ is found to be about eight times higher than its typical value of 0.0004. The charge state composition of heavy ions indicates both very hot (e.g. Fe^{+16}) and very cold (e.g. Fe^{+5}) material arriving at 1 AU. We suggest that much of the matter ejected in this CME is cold prominence material. The observed high abundance of singly-ionized helium corresponds to a freezing-in temperature of about 70,000 K, indicating that this material crosses the much hotter corona without significant additional ionization.

(29)

A Parallel Adaptive 3D MHD Scheme for Modeling Coronal and Solar Wind Plasma Flows

CLINTON P.T. GROTH, DARREN L. DE ZEEUW, TAMAS I. GOMBOSI, HAL G. MARSHALL, KENNETH G. POWELL, AND QUENTIN F. STOUT (UNIVERSITY OF MICHIGAN, ANN ARBOR MI)

A parallel adaptive mesh refinement (AMR) scheme will be described for solving the governing equations of ideal magnetohydrodynamics (MHD) in three space dimensions. This highly parallelized solution algorithm makes use of modern finite-volume numerical methodology to provide a combination of high solution accuracy and computational robustness. A flexible block-based data structure is utilized in conjunction with multi-scale domain-decomposition to facilitate automatic solution adaption using physics-based refinement criteria. The data structure and spatial decomposition procedure also enable extremely efficient and scalable implementations of the method on massively parallel computer architectures. The model has been developed on several computer platforms and extremely high parallel computational performance has been achieved (233 GFlops has been attained on a 1,024-processor Cray T3E-1200 with near-perfect scalability). Numerical results will be discussed for several idealized or model solar wind flows, including simplified representations of the background solar wind from $1 R_s$ to 0.5 AU that approximates conditions at solar minimum and coronal mass ejections (CMEs) that simulate their initiation and evolution from the solar surface out into interplanetary space. The results will demonstrate the potential of this powerful new numerical tool for enhancing our understanding of coronal physics and solar wind plasma processes, when additional and more sophisticated physical modeling, guided and tested by the results of observations, is introduced.

(30)

MHD Model of the Large-Scale Corona and the Interplanetary Medium from $1 R_\odot$ to 4 AU using SOHO and Ulysses Observations

M. GUHATHAKURTA, ¹ AND E. C. SITTLER JR. ²

¹ GSFC/CUA CODE 682, GREENBELT, MD 20771

² NASA/GSFC, 690, GREENBELT, MD 20771

A vast amount of solar coronal and interplanetary medium data have been collected over the last three solar cycles from both, space and ground-based observations which provide an excellent view of the large-scale steady state aspect of the solar corona and the interplanetary medium. Based on these data we have constructed a 2D semi-empirical MHD model of the coronal expansion and solar wind. This model assumes azimuthal symmetry and conservation of mass, momentum and energy. We make no assumptions, or simplifications of the form of heating but solve these equations for the flow velocity, effective temperature, and effective heat flux.

The input to this model is a large-scale, i) electron density distribution and ii) magnetic field geometry, for the solar corona and the interplanetary medium. The global electron density model is inferred from coronal (SOHO/LASCO/CDS and Mark III/Spartan 201) and *in situ* (Ulysses) observations.

We have taken a non-traditional approach to obtaining the solar magnetic field geometry. We use coronal observations to determine the geometry of the large-scale magnetic field, while Ulysses observations of the radial component B_r fixes the field strength at the coronal base. Significant results of our model are: 1) The model produces both slow and fast solar wind, 2) the inferred plasma parameters show good agreement with the observed parameters, both close to the Sun and at 1 AU, 3) we find that coronal white-light observations (at $2.5 R_\odot$ and beyond) alone can predict the boundary between the fast and slow solar wind, 4) a super-radial divergence is necessary to account for the gradual variation in fast solar wind observed by Ulysses from the poles down to about $25\text{-}30^\circ$ latitude, 5) magnetic field strength matches both, Ulysses observations at 1 AU and photospheric field strength at the Sun.

(31)

Plasma Properties in Coronal Funnels

P. HACKENBERG, G. MANN (ASTROPHYSIKALISCHES INSTITUT POTSDAM, POTSDAM, GERMANY)

AND E. MARSCH (MAX-PLANCK-INSTITUT FUER AERONOMIE, KATLENBURG-LINDAU, GERMANY)

A two dimensional model for the chromosphere and the corona based on the idea that the magnetic flux is strongly concentrated at the boundaries of supergranule convection cells has been proposed by Gabriel in 1976. Thus he introduced a non-trivial geometry, the so-called “funnel”, which is defined by the magnetic field lines. Since the magnetic field lines of the funnel are open field lines, the plasma is free to move along this field lines and eventually builds up the solar wind.

Based on a two dimensional funnel model we investigate the stationary plasma flow at the central line. Also heat conduction, radiative losses and a heating function are considered. The thereby found height profiles of the plasma properties within the funnel are presented.

(32)

Time dependent heating of the corona and the solar wind

VIGGO H. HANSTEEN (INSTITUTE OF THEORETICAL ASTROPHYSICS PB 1029 BLINDERN, 0315 OSLO, NORWAY)

In an effort to model the temporal variations observed in quasi-steady high-speed solar wind streams we study time-dependent models of the chromosphere – transition region – corona – solar wind system. The particle, momentum, and energy conservation equations of a hydrogen – helium plasma are solved for each ion species. The chromosphere is held at 7 000 K, and the helium abundance is specified at the base of the atmosphere. In this study the chromospheric heating is kept constant while the coronal heating is varied with time. In order to reproduce the observed variations in the solar wind parameters the coronal heating must be modulated significantly.

(33)

Inferring Coronal Hole Boundaries and Their Evolution from He I 1083 nm

KAREN L. HARVEY (SOLAR PHYSICS RESEARCH CORPORATION), AND FRANK RECELY (NOAA/SWO)

This paper will describe and illustrate how coronal holes are identified and their boundaries inferred using the NSO/KP full-disk magnetograms and He I 1083 nm spectroheliograms. Coronal holes are visible in He I 1083 nm images because this spectral line is modulated by overlying coronal radiation at wavelengths less than 50 nm, for example, low coronal emission produces areas of low He I 1083 absorption. Coronal holes can be distinguished as areas of low He I 1083 absorption (i.e., they appear bright) associated with predominately unipolar magnetic fields. The boundaries of coronal holes separate areas of low and high contrast network structures. The advantage of using He I 1083 is that coronal holes and their boundaries are not obscured by overlying coronal loops, allowing the detection of these structures near the limb and close to active regions.

We will present preliminary results of the evolution of the polar and isolated coronal holes during the minimum and early rise of cycle 23.

(34)

Coronal Hole/Streamer Interface Observed with SUMER

D.M. HASSLER (SWRI), I.E. DAMMASCH (MPAE), P. LEMAIRE (IAS), H. WARREN (NRL), K. WILHELM (MPAE)

We present observations from the SUMER instrument on SOHO of the coronal hole/streamer interface in both the north and south polar coronal hole during the Whole Sun Month (August 1996). SUMER obtained 2D spectroheliograms in the UV emission lines of Fe XII 1242 Å, Mg X 625 Å, O V 630 Å and N V 1238 Å formed over a range of temperatures corresponding to several heights in the solar transition region and corona. We specifically compare the CH/streamer interface as it appears in intensity and line width (temperature) for each of the observed emission lines.

(35)

Models of Coronal Plumes

ALAN HOOD (UNIVERSITY OF ST ANDREWS ST ANDREWS, KY16 9SS, UK)

A simple MHD model of coronal plumes will be presented. The model will focus on (i) the formation process of plumes, (ii) the energy input to plumes, (iii) the energy response of plumes and (iv) the geometrical features.

(36)

Mass Flux in the Solar Wind due to CMEs

R.A. HOWARD (E.O. HULBURT CENTER FOR SPACE RESEARCH NAVAL RESEARCH LABORATORY WASHINGTON, DC 20375)

The amount mass expelled by the Sun during a coronal mass ejection event is reexamined. Generally, a typical CME has been thought to be on the order of 10^{15} grams. In order to estimate the amount of material that continued to flow after the CME front left the field of view, various authors have assumed that the CME mass should be increased by a factor of 3. Using the wider field of view of LASCO, that the typical CME is 10^{15} grams when the CME front is located about $6-8 R_{\odot}$ (where previous coronagraphs would have measured the mass), but that the mass continues to increase another factor of 3. That is the typical CME mass is 10^{16} grams. Since the in-ecliptic mass flux due to CMEs at solar maximum has been estimated to be about 10-15% of the total mass flux, this revised estimate means that the CME mass flux during solar maximum could be nearly 50% of the total flux

(37)

CDS observations of coronal holes

JUDE INSLEY (NASA/GSFC, CODE 682.3, GREENBELT, MD 20771)

The transition from coronal hole to quiet Sun appears different depending on the wavelength of the observation. At hotter temperatures, i.e. soft X-rays, the Mg IX 368.06 EUV line, the transition is fairly marked, with an almost complete lack of emission from within the coronal hole, yet high emission from the quiet Sun. In contrast, at the cooler temperatures seen in the transition region the distinction between coronal hole and quiet Sun becomes much harder, the chromospheric network structure being equally visible inside and out of the coronal hole. CDS observations of the coronal hole/quiet Sun interface are presented, with a look at the changes over time, and with temperature.

(38)

Temporal Behavior of Solar Wind Fe and O in High Speed Stream Onsets

F. M. IPAVICH (1), G. GLOECKLER (1,2), T. H. ZURBUCHEN (2), S. HEFTI (2), P. BOCHSLER (3), L. A. FISK (2), R. KALLENBACH (4), J. A. PAQUETTE (1), R. F. WIMMER-SCHWEINGRUBER (3)

(1) UNIVERSITY OF MARYLAND, COLLEGE PARK, MD 20742, USA

(2) THE UNIVERSITY OF MICHIGAN, SPACE RESEARCH BUILDING, ANN ARBOR, MI 48109, USA

(3) UNIVERSITY OF BERN, PHYSIKALISCHES INSTITUT, SIDLERSTRASSE 5, CH-3012 BERN, SWITZERLAND

(4) INTERNATIONAL SPACE SCIENCE INSTITUTE, CH-3012 BERN, SWITZERLAND

Most well-defined coronal hole-associated high speed solar wind streams are preceded by a region of enhanced density. This density pile-up region is followed by relatively gentle increases in speed and kinetic temperature. Here we concentrate on the solar wind properties in the pile-up region, using charge state data from the SWICS sensor on the ACE spacecraft, the elemental abundance ratios measured by both ACE/SWICS and the CELIAS/MTOF sensor on the SoHO spacecraft, and isotopic ratios from SoHO/MTOF. We also explore the question of whether the heavy ion isotopic composition differs in solar wind flows of coronal hole and non-coronal hole origin.

(39)

He I 1083 nm Asymmetry and EUV Line Shifts in Coronal Holes

HARRISON P. JONES (NASA/GODDARD SPACE FLIGHT CENTER), VINCENZO ANDRETTA (NASA/GODDARD SPACE FLIGHT CENTER), AND MATTHEW J. PENN (NATIONAL SOLAR OBSERVATORY)

Dupree, Penn, and Jones (1996, ApJ 467, L121) reported observations taken at the National Solar Observatory/Kitt Peak Vacuum Telescope (NAO/KPVT) with the NASA/NSO spectromagnetograph of blue-wing asymmetries in the He I 1083.0 nm line in two polar coronal holes. The authors pointed out that these data could indicate outwardly directed flows consistent with an origin of the high-speed solar wind in the low transition region. By contrast, Warren, Mariska, and Wilhelm (1997, ApJ 490, L187) discuss spectral observations obtained with SOHO/SUMER which show no evidence of relative blue shifts in a coronal hole in cool transition-region lines. Without resolving this apparent discrepancy, we report here further observations of He I 1083.0 nm asymmetry, discuss analysis techniques and instrumental effects, and show one instance (17 Jan 97) of coordinated observations with the SOHO/Coronal Diagnostics Spectrometer (CDS). After interpolation to compensate for curvature, tilt, and skew of the CDS spectra with respect to the detector, we have used two independent techniques to derive line-of-sight velocities. With both methods we find systematic blue shifts in the coronal hole relative to other areas in the CDS field of view in the following cool transition-region lines: He I 58.4 nm, He II 30.4 nm, and O V 63.0 nm. The signal in other spectral lines observed with CDS was too noisy for a reliable wavelength determination by either method. The 1083.0 nm observations show blueward asymmetry in the same coronal hole during the same time interval, although the spatial correspondence with the CDS data is general, not detailed. This might result from the different spatial scanning patterns and data accumulation rates between the two instruments, and investigation of this possibility is in progress.

(40)

Study of Dynamical Properties of Coronal Structures in the Polar Regions

M. KAROVSKA, B. WOOD, J. W. COOK, G. E. BRUECKNER (HARVARD-SMITHSONIAN CENTER FOR ASTROPHYSICS), G. E. BRUECKNER, J. W. COOK (NAVAL RESEARCH LABORATORY)

We present the results from a study of the dynamical properties of coronal structures in the Sun's polar regions using SOHO/LASCO C1 and C2 coronagraph observations. The data set includes C1 observations in the Fe XVI line and the nearby continuum, and C2 polarized light observations. The temporal cadence in different observations varies from 1 minute to more than 20 minutes between images. Image enhancement techniques were applied to the data to extract the low contrast coronal structures which allowed better identification of the plumes, the interplume regions, and other structures in the corona. In selected sectors corresponding to different regions we measured intensity as a function of height above the limb. Based on the evolution of the intensity as a function of time, we measured the speed of the outflow in different coronal hole regions. We compare these results to the velocities measured using the observations carried with other SOHO instruments, including UVCS and EIT. The data set includes a sequence of LASCO/C2 images of the north polar region from 1997 March 22, which lasted for about 41 hours and had an average time cadence of 12 minutes. Near the end of the sequence, a series of three compact jets of material were ejected from a point near the north pole. We estimate the outflow speed of these jet-like structures to be about 350 km/s.

(41)

Numerical simulations of stellar winds

R. KEPPENS AND J. P. GOEDBLOED

We discuss steady-state transonic outflows obtained by direct numerical solution of the hydrodynamic and magnetohydrodynamic equations. We make use of the Versatile Advection Code, a software package for solving systems of (hyperbolic) partial differential equations. We model thermally and magneto-centrifugally driven stellar outflows as generalizations of the well-known Parker and Weber-Davis wind solutions. To obtain steady-state solutions efficiently, we exploit fully implicit time stepping.

We emphasize the boundary conditions imposed at the stellar surface. For axisymmetric wind solutions, we address issues associated with the equivalent analytical description for axisymmetric, stationary MHD equilibria. The latter involves the combined solution of the mixed-type partial differential equation governing the cross-fieldline force balance, with the algebraic condition expressed by the Bernoulli equation. The numerical solutions of the MHD equations can then be verified using the knowledge of the flux functions.

(42)

On the coronal electron temperature profile and coronal heating constrained by in-situ observations

Y.-K. KO (HARVARD-SMITHSONIAN CENTER FOR ASTROPHYSICS, CAMBRIDGE, MA 02138)
AND C. P. T. GROTH (DEPARTMENT OF ATMOSPHERIC, OCEANIC AND SPACE SCIENCES,
UNIVERSITY OF MICHIGAN, ANN ARBOR, MI 48109)

The electron temperature profile in the polar coronal hole inferred by the solar wind ionic charge state data exhibits a local maximum of about 1.5 million degrees (Ko et al. 1997). This indicates the existence of electron heating in the inner coronal region. In this paper, a two-fluid solar wind model, which incorporates additional 'mechanical' heating, is used to investigate the heating of the electrons in the coronal hole. We find that the classical collision-dominated expressions for the electron conduction heat flux are not strictly valid and need to be severely limited in order for the electron temperatures predicted by the model to agree with constraints supplied by both the solar wind ionic charge state data and the solar wind plasma properties observed at 1 AU. The corresponding constraints on the magnitude of the coronal heating will also be discussed.

(43)

UVCS/SOHO Observations of Spectral Line Profiles in Polar Coronal Holes

J. L. KOHL, S. FINESCHI, R. ESSER, A. CIARAVELLA, S. R. CRANMER, L. D. GARDNER,
A. MODIGLIANI, R. SULEIMAN, AND G. NOCI

The SOHO Ultraviolet Coronagraph Spectrometer (UVCS/SOHO) is being used to measure spectral line profiles in polar coronal holes. The measurements include HI 121.6 nm, O VI 103.2 nm and 103.7 nm and Mg X 62.5 nm. Measurements of O VI profiles above $2.2 R_{\odot}$ and Mg X profiles above $1.75 R_{\odot}$ are presented for the first time. The measurements are used to determine the velocity distribution of the corresponding ions along the lines-of-sight. The velocities are much different for the various particles with O^{5+} having the largest most

probable speeds at heliocentric heights above $1.8 R_{\odot}$. Mg^{9+} is found to have most probable speeds above $1.8 R_{\odot}$ that fall between those of O^{5+} and the smaller H^0 values. The derived velocity distributions for O^{5+} and Mg^{9+} do not appear to be dominated by transverse wave motions. The possibility that the velocity distributions are caused by ion cyclotron resonance with high frequency MHD waves is being investigated. Some details of the observations and the use of the UVCS instrument will be presented. Information for gaining access to UVCS data and the data analysis software as well as information about how to arrange for specialized UVCS observations will also be presented. This work is supported by the National Aeronautics and Space Administration under grant NAG5-3192 to the Smithsonian Astrophysical Observatory, by Agenzia Spaziale Italiana, and by Swiss funding agencies.

(44)

The highest solar wind velocity in a polar region estimated from IPS tomography analysis

M. KOJIMA, T. OHMI, A. YOKOBE, M. TOKUMARU (SOLAR-TERRESTRIAL ENVIRONMENT LABORATORY, NAGOYA UNIVERSITY 3-13 HONOHARA, TOYOKAWA 442-8507, JAPAN), AND K. HAKAMADA (DEPARTMENT OF ENGINEERING PHYSICS, CHUBU UNIVERSITY KASUGAI, AICHI 487, JAPAN)

The Ulysses has revealed that a high-speed wind increases its velocity gradually with latitude. We have investigated how the velocity increase continues to a polar region and at which distance the gradual velocity increase at high latitudes is formed. For this purpose we have made tomography analysis of the latitudinal structure of the solar wind speed using interplanetary scintillation data obtained at heliocentric distances of 0.2-0.9 AU in 1996. Firstly we have confirmed the validity to use the IPS tomography for this study by obtaining a quite similar gradual velocity increase to that observed by the Ulysses. The analysis obtained that the velocities in the polar regions are around 800 km/s during the Carrington rotations of 1908-1911, and that in rotations of 1911-1915 they are about 900 km/s. These velocities are on linear extrapolation from the gradual velocity increase at 30-80 degrees or slightly higher than the extrapolation. Neither large increase nor drop from the linear extrapolation was obtained. These facts that the IPS observed the gradual velocity increase at 0.2-0.9 AU indicate that it is not formed during long distance propagation to the Ulysses, but is formed within a distance of 0.2 AU. We therefore expect that the cause will be found in distance range of SOHO observations.

(45)

Maps of the Coronal Electron Density from LASCO-C2 Images

P. LAMY, E. QUEMERAIS, M. BOUT AND A. LLEBARIA

No abstract submitted.

(46)

Observation of transition region fine structures with SUMER and CDS

ENRICO LANDI (UNIVERSITÀ DI FIRENZE, ITALY DIPARTIMENTO DI ASTRONOMIA E SCIENZA DELLO SPAZIO, LARGO E.FERMI 5, 50125, FIRENZE, ITALY)

We present an investigation on transition region fine structures using Oxygen, Silicon, Nitrogen and Neon lines observed with SUMER and CDS over a large quiet Sun area. The observed region shows a large number of bright points in these lines associated with upflows, jet-like features. Some modeling of some of these active points is presented. Also Hydrogen continuum absorption is investigated through the comparison of SUMER-CDS spectral lines.

(47)

Loop models with SOHO observations

ENRICO LANDI AND MASSIMO LANDINI (DEPARTMENT OF ASTRONOMY, UNIVERSITY OF FLORENCE, ITALY)

In the present work we use SOHO CDS, MDI and EIT active region observations in order to measure the electron temperature, density and pressure of active region loops. These measurements are used to build empirical models of loops, which are compared with theoretical models from Landini and Monsignori Fossi (1975). Energy balance for the loop model is investigated in order to determine the temperature dependence of the heating function.

(48)

Search for signatures of a coronal hole in transition region lines near disk center

P.LEMAIRE, K. BOCCHIALINI, V. ALETTI, D. HASSLER, K. WILHELM (IAS, ORSAY - FRANCE; SWRI, BOULDER- UNITED STATES; MPAE, LINDAU - GERMANY)

The analysis of a set of data taken by SUMER near disk center, where a small coronal hole is detected from EIT images, is performed. From the measurements of doppler velocities, non-thermal velocities and intensities, we search for the diagnostics and the signature of the small scale structures in the coronal hole in using transition region lines.

(49)

Heating and Cooling of Protons by Turbulence-Driven Ion Cyclotron Waves in the Fast Solar Wind

XING LI, SHADIA R. HABBAL, RUTH ESSER (HARVARD-SMITHSONIAN CENTER FOR ASTROPHYSICS, CAMBRIDGE, MA 02138)

JOSEPH V. HOLLWEG (UNIVERSITY OF NEW HAMPSHIRE, DURHAM, NH 03824)

The heating, cooling and acceleration of protons by parallel propagating nondispersive ion cyclotron waves in the fast solar wind are investigated. Low frequency Alfvén waves are assumed to carry most of the energy needed to accelerate and heat the fast solar wind. Nonlinear cascade processes, namely the Kolmogorov and Kraichnan dissipation of Alfvénic turbulence, are utilized to transport energy from the low frequency waves to the ion cyclotron resonant range where it is picked up by the plasma through the resonant cyclotron interaction. The turbulence determines the net dissipation, while the resonant interaction determines how the heat is distributed between the parallel and perpendicular degrees of freedom. Ion cyclotron waves are found to be able to substantially heat protons in the direction perpendicular to the magnetic field. At the same time these waves can heat or cool protons in the parallel direction depending on the degree of anisotropy. While the cooling in the parallel direction is

the dominant effect, the heating in the parallel direction becomes important when $T_{p\perp} \gg T_{p\parallel}$ and occurs in our models at intermediate distances between 1.5 and 40 R_s . Ion cyclotron waves not only cause a strong proton temperature anisotropy in the inner corona but also limit the growth of the proton temperature anisotropy in interplanetary space. Both Kolmogorov and Kraichnan dissipation rates yield $T_{p\perp} \gg T_{p\parallel}$ in the corona in agreement with inferences from recent ultraviolet coronal measurements, and predict temperatures at 1AU which match in situ observations. The large coronal $T_{p\perp}$ is able to rapidly accelerate the solar wind close to the Sun. However, these mechanisms yield electron temperatures which are too low, implying that they do not account for the energy needed to heat the electrons and protons in the region where radiation losses are still significant.

(50)

Hybrid Simulations of Wave Propagation and Ion Heating in the Solar Wind using a 1D Expanding Box Model

P. C. LIEWER, M. VELLI AND B. E. GOLDSTEIN (JET PROPULSION LABORATORY, CALTECH, PASADENA, CA 91109)

We present results from the first hybrid simulations of the evolution of Alfvén waves close to the ion cyclotron frequency in the solar wind, which take into account the basic properties of the background solar wind flow, i.e., the effects of expansion and the variation of the cyclotron frequency with distance from the Sun. We follow the evolution of a collection of ions of multiple species in a frame of reference moving with the solar wind using a new 1D expanding box hybrid model. This model is related to a previous MHD model (Grappin and Velli, 1993), which allows the use of a simple cartesian geometry with periodic boundary conditions. The use of stretched expanding coordinates in directions transverse to the mean radial solar wind flow naturally introduces an anisotropic damping effect on velocity and magnetic field, and the Parker-like rotation of the average magnetic field. Using the expanding box approximation in a hybrid code allows us to couple the effects wave-particle interactions and solar wind expansion self-consistently. We will show how this affects the 1-d evolution of an initially circularly polarized large amplitude Alfvén wave in parallel and oblique propagation. For example, we will investigate the evolution of waves with frequencies which are originally below the ion cyclotron frequency, but which come into resonance as the solar wind expands. Cases with both a single ion species and multiple ion species will be presented.

[1] R. Grappin and M. Velli, JGR 101, 425 (1996).

(51)

Density and Electron Temperature in Coronal Streamers

LISA MACCARI AND THE UVCS TEAM (UNIVERSITÀ DI FIRENZE - SMITHSONIAN ASTROPHYSICAL OBSERVATORY)

The UVCS has observed coronal streamers with the purpose of determining the physical parameters of these structures. We have focussed our attention on a streamer observed on July 23-27, 1997, in particular on the total intensity of the first lines of the Lyman series of H I, chiefly Ly-alpha and Ly-beta. The comparison of these quantities makes it possible to separate the collisional from the radiative component of the lines, and thus determine the density (averaged over the line of sight) of the electrons and of the neutrals. From these, and from hydrogen ionization calculations, it is possible to obtain an indirect determination of the electron temperature. We report on these studies and discuss the significance of the values obtained.

(52)

Solar wind models from the Sun to 1 AU: Constraints by “in situ” and remote sensing measurements

E. MARSCH (MAX-PLANCK-INSTITUT FUER AERONOMIE, MAX-PLANCK-STR. 2, D-37191
KATLENBURG-LINDAU, GERMANY)

There are three major types of solar wind: The steady fast wind originating on open magnetic field lines in coronal holes, the unsteady slow wind coming from the temporarily open streamer belt and the transient wind in the form of coronal mass ejections. Models for these types of wind have been developed to different levels of sophistication. The majority of the models is concerned with the fast wind, which is, at least during solar minimum, the normal mode of the wind and most easily reproducible in its properties by multi-fluid models involving waves. A tutorial review of some relevant models is given with emphasis on the fast wind. The in-situ constraints imposed on the models, mainly by the Helios (in ecliptic) and Ulysses (high-latitude) interplanetary measurements, are extensively discussed with respect to fluid and kinetic properties of the wind. The recent SOHO observations have brought a wealth of new information on the boundary conditions for the wind in the inner solar corona and on the plasma conditions prevailing in the transition-region and chromospheric sources of the wind plasma. These results are presented, and then some key questions and scientific issues are identified for the subsequent in-depth discussions in the working groups.

(53)

Energy and Momentum Deposition in Coronal Holes – Solar Coronal Hole Simulations Compared with Interpretations of Yohkoh-SXT and SOHO-UVCS Observations

P. C. H. MARTENS, K. TZIOTZIOU, AND A. G. HEARN

A grid of 74 time dependent coronal models with parametrized heating distribution, representing a wide range of physical parameters, has been calculated (Tzotziou, Martens & Hearn, A&A 1998, submitted). We find that three of these models reproduce observations made by Hara et al. (1994) with the soft X-ray telescope aboard Yohkoh, which indicate a temperature of about 1.8 million Kelvin with an emission measure of $10^{25.5}$ to $10^{26.2}$, while other models reproduce the more standard Yohkoh and Skylab observations, indicating a temperature of about 1.4 million Kelvin.

The best fit for the high coronal temperature and emission measure gives a velocity at the Earth's orbit of only 10 km/s. A model including acceleration by Alfvén waves gives a final velocity of 630 km/s which is in agreement with the observations. The mechanical heating flux at the transition region is $2.1 \cdot 10^5$ erg/cm²/s with a weighted average dissipation scale length of $0.1 R_{\odot}$. The flux of Alfvén waves is 10^5 erg/cm²/s.

In our models the velocity of the solar wind from coronal holes is completely determined by Alfvén wave acceleration, in contrast to previous models in which the Alfvén wave acceleration increased the velocity of the purely thermal wind only by a factor 2.

Observations of the non thermal broadening of the coronal red and green lines are consistent with this model, and the compatibility of these results with the very recent observations of line broadening and Doppler dimming by UVCS onboard SOHO is being studied. We expect to present preliminary results of that comparison at the meeting.

(54)

Source of the Equatorial Plasma Sheet at Solar Minimum

D. J. MICHELS (NAVAL RESEARCH LABORATORY, WASHINGTON, DC 20375-5352, USA)

M. J. KOOMEN (SAKS FREEMAN, INC. / NAVAL RESEARCH LABORATORY WASHINGTON, DC 20375-5352, USA)

S. P. PLUNKETT (UNIVERSITIES SPACE RESEARCH ASSOCIATION / NAVAL RESEARCH LABORATORY, WASHINGTON, DC 20375-5352, USA)

S. PASWATERS (INTERFEROMETRICS, INC. / NAVAL RESEARCH LABORATORY, WASHINGTON, DC 20375-5352, USA)

S.T. WU AND A.-W. WANG (UNIVERSITY OF ALABAMA AT HUNTSVILLE, HUNTSVILLE, AL 35899, USA)

EIT and LASCO images of the quiescent corona, recorded during the early months of the SOHO Mission, show that the solar minimum corona is highly structured close to the Sun, but less so at greater distances. The polar open-field regions are characterized by high magnetic pressure. They exert a strong compressive force on plasma emitted from lower-latitude regions, where the field lines are predominantly closed loops. Within these closed-field regions, a three-tiered hierarchy of loop scales has been discerned. The observations are consistent with a three-dimensional axisymmetric MHD numerical model that takes account of interactions between multiple bipolar magnetic regions at mid latitudes.

(55)

Physical Properties of Coronal Hole/Streamer boundaries, and adjacent regions as observed by Spartan 201

MARI PAZ MIRALLES¹, LEONARD STRACHAN¹, LARRY D. GARDNER¹, PETER L. SMITH¹, JOHN L. KOHL¹, MADHULIKA GUHATHAKURTA^{2,3}, AND RICHARD R. FISHER²

¹ HARVARD-SMITHSONIAN CENTER FOR ASTROPHYSICS, 60 GARDEN STREET, MS 50, CAMBRIDGE, MA 02138

² NASA GODDARD SPACE FLIGHT CENTER, CODE 682, GREENBELT, MD 20771

³ PHYSICS DEPARTMENT, THE CATHOLIC UNIVERSITY OF AMERICA, D. C.

The Spartan 201 flights from 1993 to 1995 provided us with observations in HI Lyman- α of several coronal hole/streamer boundaries and adjacent streamers during the declining phase of the current solar cycle. The analysis of the data allows us to derive physical and morphological characteristics for the observed regions. We compare streamer and boundary properties derived from the observations in order to characterize hydrogen velocity distributions. We also compare UVCS/Spartan HI Lyman- α and WLC/Spartan White Light observations to obtain constraints on the geometry of coronal hole/streamer boundaries over a two year period.

This work is supported by NASA under Grant NAG 5-613 to the Smithsonian Astrophysical Observatory.

(56)

Coronal Heating by Magnetic Explosions

R. L. MOORE, D. A. FALCONER, J. G. PORTER, S. T. SUESS (NASA/MSFC)

We build a case for the persistent strong coronal heating in active regions and the pervasive quasi-steady heating of the corona in quiet regions and coronal holes being driven in basically the same way as the intense transient heating in solar flares: by explosions of sheared magnetic fields in the cores of initially closed bipoles. We apply a magnetic-configuration framework for flares and coronal mass ejections to the strong coronal heating observed by the Yohkoh Soft X-ray Telescope in an active region with strongly sheared core fields observed by the MSFC vector magnetograph. All of the strong coronal heating is in continually microflaring sheared core fields or in extended loops rooted against these active core fields. Thus, the strong heating is in field configurations appropriate for the heating to be driven by frequent core-field explosions that are smaller but similar to those in confined flares and flaring arches. From analysis of the thermal and magnetic energetics of two selected core-field microflares and a bright extended loop, we find that it is energetically feasible for the sheared core fields to drive all of the coronal heating in the active region via a staccato of magnetic microexplosions. We then point out that (1) the field configurations for strong coronal heating in our example active region (i.e., neutral-line core fields, many embedded in the feet of extended loops) are present in abundance in the magnetic network in quiet regions and coronal holes, and (2) it is known that many network bipoles do microflare and that many produce detectable coronal heating. We therefore propose that exploding sheared core fields are the drivers of most of the heating and dynamics of the solar atmosphere, ranging from the largest and most powerful coronal mass ejections and flares, to the vigorous microflaring and coronal heating in active regions, to a multitude of fine-scale explosive events in the magnetic network, driving microflares, spicules, global coronal heating, and, consequently, the solar wind.

(57)

SOHO Observations of Density Fluctuations in the Solar Wind

L. OFMAN (RAYTHEON STX AND NASA GODDARD SPACE FLIGHT CENTER, MAIL CODE 682, GREENBELT, MD 20771, USA)

M. ROMOLI (DEPARTMENT OF ASTRONOMY AND SPACE SCIENCE, UNIVERSITY OF FLORENCE, LARGO FERMI 5, 50125 FLORENCE, ITALY)

G. POLETTI (ARCETRI OBSERVATORY, I-50125 FLORENCE, ITALY)

G. NOCI (DEPARTMENT OF ASTRONOMY AND SPACE SCIENCE, UNIVERSITY OF FLORENCE, LARGO FERMI 5, 50125 FLORENCE, ITALY)

J. L. KOHL (HARVARD-SMITHSONIAN CENTER FOR ASTROPHYSICS, 60 GARDEN ST, CAMBRIDGE, MA 02138, USA)

R. A. HOWARD (NRL, CODE 7660, WASHINGTON, DC 20375)

C. ST. CYR (NRL, CODE 7660, WASHINGTON, DC 20375)

C. DEFEST (STANFORD UNIVERSITY, AND NASA GODDARD SPACE FLIGHT CENTER, CODE 682.3, GREENBELT, MD 20771)

In recent UVCS/SOHO White Light Channel (WLC) observations we found quasi-periodic variations in the polarized brightness (pB) in the polar coronal holes at heliocentric distances

of 1.9-2.45 solar radii. The motivation for the observation is the 2.5D MHD model of solar wind acceleration by nonlinear waves, that predicts compressive fluctuations in coronal holes (Ofman and Davila 1997; 1998). Fourier power spectrum of the polarized brightness (pB) time series shows significant peaks at about 10 minutes (after correcting for the transmission delay time) and possible fluctuations on longer time scales (Ofman et al. 1997). In February 1998 we performed new observations using the UVCS/WLC in the coronal hole and obtained additional data. The new data corroborates our earlier findings with higher statistical significance. The new longer observations show that there are several peaks in the power spectrum close to the 10-12 minute range. These timescales agree with EIT observations of brightness fluctuations in polar plumes (DeForest and Gurman 1997). We performed preliminary LASCO/C2 observations in an effort to further establish the coronal origin of the fluctuations.

(58)

A study of solar wind acceleration based on the gyro-tropic transport equations

E. L. OLSEN (CENTER FOR ASTROPHYSICS, HARVARD UNIVERSITY, CAMBRIDGE, USA; NOW AT STATOIL, STAVANGER, NORWAY, - ELOLS@STATOIL.COM)

E. LEER (INSTITUTE OF THEORETICAL ASTROPHYSICS, UNIVERSITY OF OSLO, PO Box 1029, N-0316 OSLO, NORWAY, - EGIL.LEER@ASTRO.UIO.NO)

The gyro-tropic transport equations are used to describe the outflow of an electron-proton gas in an expanding magnetic field, from the inner corona and out to 30 solar radii. The coronal energy input is specified, and we solve for the electron density, flow speed along the magnetic field, parallel and perpendicular temperatures, and the “parallel” and “perpendicular” heat flux densities along the field. We have studied models with ion-cyclotron heating of the inner corona as well as models where some of the energy flux is in the form of low frequency waves that “push” the flow. In order to obtain coronal “temperatures” that are in agreement with the UVCS/SOHO observations of the 1216 Å line in coronal holes, a significant fraction of the energy flux must be in the form of low frequency waves that accelerate the solar wind without heating the inner corona.

(59)

Study of coronal rotation by solar radio flux measurements

HARI OM VATS, M.R. DESHPANDE, M. MEHTA (1), K.J. SHAH AND C.R. SHAH (PHYSICAL RESEARCH LABORATORY, AHMEDABAD-380009, INDIA)

(1) J.J. SCIENCE COLLEGE, NADIAD, INDIA

Heliosesmology measurements have begun to provide a picture of Sun’s angular velocity as a function of both depth and latitude. The rate of improvement in this picture has been fast and is likely to be so for near future. This has potential to provide a nearly complete picture of the rotation throughout solar interior. The rotation of the solar photosphere is usually measured by tracking the tracers e.g. sunspots, faculae, low-level magnetic features etc. Most of these imply an equatorial sidereal rotation period of 25 days and a polar period of about 34 days. Solar coronal rotation is relatively less known . We recently attempted fractal analysis of radio emission from solar corona and found that the time series of radio emission at several frequencies can be easily used for determining the rotation of solar corona. The study reveals several interesting features about the rotation of solar corona. Solar corona rotates faster than the photosphere. It is not possible to investigate latitudinal variation of solar coronal rotation

by this method, however it is certainly possible to investigate temporal changes in the rotation. It is found that coronal rotation period varies during the different phases of the solar cycle. Here the results of auto and cross correlation analysis for solar cycles 21 nad 22 will be presented and compared with those by other methods.

(60)

Determination of the Flux of matter in a polar coronal hole via coordinated observations between SOHO/SUMER and ground during the 1998 total eclipse

SPIROS PATSOURAKOS (I.A.S. UNIVERSITE PARIS XI BAT 121)

Polar coronal holes represent the most convincing site of the origin of the high-speed solar wind. A precise knowledge of the flux of matter at the coronal base is extremely important in placing constraints on wind models. White-light eclipse-observations still remain an excellent way to determine the electronic density in the low solar corona. Here we combine high-accuracy Doppler shifts measured in O VI (1037.6 Å) line obtained by SUMER with electronic densities measured in WL – during the 26 Feb 1998 eclipse – in the vicinity of the south coronal hole.

(61)

MHD Modeling of the Polar Solar Wind Acceleration

YU.V. PISANKO (INSTITUTE OF APPLIED GEOPHYSICS, ROSTOKINSKAYA ST.9, MOSCOW 129128, RUSSIA)

Recent remote observations of the polar corona on board of the SOHO spacecraft (presentations at the 5th SOHO Workshop by Kohl et al. and Brueckner et al.) have detected the rapid polar solar wind acceleration on the first few solar radii above the solar surface.

An attempt is made to propose an MHD model taking into account the rotation of the magnetic Sun as an expansion under the inverted Rossby number to describe these acceleration regimes from the united position. The model (Habbal & Tsinganos, 1983, JGR, 88, 1965) of the steady isothermal solar wind with momentum deposition allowing a continuous (Parker's) solution as well as solutions with shock discontinuities is used as zero-order approximation (absence of rotation). The rotation induced effects, i.e. the double electric layer in the polar corona and the system of field-aligned electric currents above the double layer creating the additional pressure gradient and hence the additional polar solar wind acceleration are taken into account in the first-order approximation (slow rotation).

In the framework of this approach i) the empirical polar solar wind acceleration curve derived from H I Ly alpha emission line intensity measurements from the SOHO UVCS (Kohl et al.) can be simulated when a continuous (Parker's) solution is used as zero-order approximation; ii) SOHO LASCO observations of high (terminal) polar solar wind velocities close to the solar surface (Brueckner et al.) can be simulated when a discontinues solution with shock transition is used as zero-order approximation. In accordance with (Habbal & Tsinganos) the realization of each acceleration regime depends on the previous temporal evolution of the flow.

(62)

Velocity shear induced effects in the solar wind

S. POEDTS (1), A. ROGAVA (1,2), AND S. M. MAHAJAN (3)

(1) CENTRE FOR PLASMA ASTROPHYSICS, K.U.LEUVEN, CELESTIJNENLAAN 200B, 3001 HEVERLEE, BELGIUM

(2) ABASTUMANI ASTROPHYSICAL OBSERVATORY, TBILISI, REPUBLIC OF GEORGIA

(3) INSTITUTE FOR FUSION STUDIES, THE UNIVERSITY OF TEXAS AT AUSTIN, U.S.A.

Recent studies showed that velocity shear is an important physical aspect that may influence the solar wind dynamics considerably. In particular, the sheared background flow in the solar wind plasma induces coupling between the different MHD wave modes, i.e. Alfvén waves (AW) and fast (FMW) and slow (SMW) magnetosonic waves, resulting in their mutual transformations with corresponding energy redistribution between the modes. As a consequence, the sheared solar wind flow opens *two channels for energy transfer*, viz. *from one wave mode to the other*, but also *from and to the background flow*. It is shown that the shear flow induced wave coupling and energy transfer mechanisms operate *close to optimal efficiency* under solar wind conditions. This could have some interesting effects on the solar wind dynamics with direct consequences for some longstanding puzzles, e.g.:

- it is demonstrated that the long-period Alfvén waves observed in the solar wind at $r > 0.3$ AU can be generated by much faster periodic oscillations in the photosphere;
- it is also shown that the FMWs transfer a part of their energy to the background wind flow while they are converted into AWs and/or SMWs, resulting in the acceleration of solar wind particles;
- the mutual energy transfers generate beat modes in the solar wind which may be an observable signature that can confirm the existence of velocity shear induced processes in the solar wind.

(63)

Energetics of the Lower Transition Region

A. I. POLAND AND J. CHAE

We address the question of how non-LTE radiative losses and partial ionization of H and He affects the energetics and structure of the solar transition region. To accomplish this we have constructed theoretical models of a thin rigid magnetic flux tube with a steady material flow, which is embedded vertically in the solar atmosphere. These models include the effects of material flow, conduction, non-LTE radiative transfer in H and He, and partial ionization. We find that the effect of non-LTE is significant near the base of the transition region at temperatures less than 1.5×10^4 K. This leads to a 1 order of magnitude increase in the differential emission measure in comparison with the optically thin approximation with complete ionization in the low temperature regime. Above this region the non-LTE and opacity effects are small. In the upflow case the conductive and convective energy processes dominate to such a large extent that non-LTE radiative processes and partial ionization are not important.

We also clearly demonstrate, confirming the work of other authors, why the observations of the chromosphere transition region show a strong predominance of downflowing material. This result is presented in a manner that makes the result easily understandable.

(64)

Microflares and the Heating of Plumes Over Enhanced Network

J. G. PORTER, D. A. FALCONER, AND R. L. MOORE

Previous work has shown that extended magnetic loops arising from active regions on the Sun have especially active islands of included polarity at their feet (e.g., Falconer et al 1997; Porter, Falconer, and Moore 1998). Frequent microflaring in the low-lying fields of these footpoint sites is possibly the cause of the enhanced heating of the higher structures, although detailed comparison of the intensity variations in the low and high structures raises other possibilities (though the extended heating appears to be driven from around the island in any case). Similarly, in the quiet Sun, extended loops arise from near compact bright bipolar areas in the magnetic network, and arch along the network or across supergranular cells (Falconer et al. 1998). In this work with SOHO/EIT data, we present examples of very high extended magnetic structures, possibly open, likewise rooted at sites of mixed polarity in enhanced network. These magnetic footpoint conditions are consistent with those for polar coronal hole plumes noted by Wang et al 1997. We examine the intensity variations in these high structures and in the bipolar regions at their feet for clues to the heating mechanism(s) involved in maintaining these plumes.

Falconer, D.A., Moore, R.L., Porter, J.G., Gary, G.A., and Shimizu, T. 1997, ApJ 482, 519.

Falconer, D.A., Moore, R.L., Porter, J.G., and Hathaway, D. 1998, ApJ, in press.

Porter, J.G., Falconer, D.A., and Moore, R.L. 1998, in Solar Jets and Coronal Plumes, ed. T. Guyenne, ESA SP-421 (ESTEC, The Netherlands), in press.

Wang, Y.-M. et al 1997, ApJ 484, L75.

(65)

Composition and Elemental Abundance Variations in the Solar Corona Solar Atmosphere and Solar Wind

JOHN C. RAYMOND

Order of magnitude variations in the relative abundances are observed in the solar corona and solar wind. The instruments aboard SOHO make it possible to explore these variations in detail to determine whether they arise near the solar surface or higher in the corona. First Ionization Potential (FIP) effect is clearly seen, and that must arise in the chromosphere, while from gravitational settling is observed at larger heights in quiescent streamers.

(66)

Velocity of Toroidal Magnetic Clouds From the Sun to the Earth's Orbit

EUGENE ROMASHETS (IZMIRAN, TROITSK, MOSCOW REGION, 142092 RUSSIA)

Using approach described in Romashets, 1994 we have constructed velocity profiles of toroidal clouds for different parameters of ambient solar wind and cloud. We considered two possible

orientations of the cloud: with the plane of torus parallel and perpendicular to the line Earth-Sun. Some additional assumption about cloud's expansion were used. The obtained results were tested on data about May 14-17, 1998 magnetic cloud.

(67)

Electron Densities measured with UVCS/WLC

M. ROMOLI ET AL.

The White Light Polarimeter (WLC) of the Ultraviolet Coronagraph Spectrometer (UVCS) on board of the Solar Heliospheric Observatory (SOHO) is a coronagraph polarimeter that measures the polarized brightness (pB) of the K-corona between 1.6 and 5 R_{\odot} in the 450–600 nm wavelength range. The pB gives a direct measurement of the electron density integrated along the line of sight (LOS), which is a key parameter for coronal plasma diagnostics.

The WLC observations, combined with the UVCS ultraviolet spectrometers observations, provide an unprecedented diagnostic tool for densities, temperatures and velocities of the plasma in the extended corona. This paper is devoted to the determination of the electron density in coronal holes based on the UVCS synoptic observation and on special observation with higher radial scanning resolutions.

(68)

Signatures of coronal hole spectra between 700 and 1500 Angstrom measured with SUMER on SOHO

U. SCHUEHLE, W. CURDT, S. SOLANKI, K. STUCKI, AND K. WILHELM

With the SUMER instrument on SOHO a spectral atlas of the full spectral range of the instrument is performed regularly in quiet Sun areas on the solar disk. More rarely such an atlas has been measured at coronal hole locations. We present such spectra taken at locations where part of the spectrometer slit intersects quiet Sun and either a polar coronal hole or an equatorial coronal hole area. By comparison of the line intensities between the parts of the spectrum taken inside the holes and the one in the quiet Sun we work out the signatures of the specific coronal hole in the chromosphere, transition region and lower corona. Besides a generally lower emission inside the coronal hole area we find that, out of many hundred lines in the spectra, only very few show distinctly different intensity ratios which we discuss in relation to the formation temperatures of the emitting species. The results give us new criteria for the characterization of coronal holes.

(69)

The rotation of the solar corona - an analysis of LASCO Fe XIV emission data during solar minimum activity

R. SCHWENN, B. INHESTER, B. PODLIPNIK, N. SRIVASTAVA, G. STENBORG (MAX-PLANCK-INSTITUT FUER AERONOMIE, D 37191 KATLENBURG-LINDAU, GERMANY)

We analyse data observed by the LASCO C1 coronagraph on board the SOHO spacecraft during the solar minimum activity 1996. Using different techniques, we investigate the periodicity and recurrence of Fe XIV emission structures as functions of heliospheric latitude and distance above

the sun's surface. Since the FeXIV emission is due to hot coronal plasma on presumably closed field lines we are confident that our analysis allows to draw conclusions about the rotation of the coronal streamer belt plasma. Particular emphasis is put on the yet unsolved question of how the differential rotation of the Sun's surface is transmitted into the corona.

(70)

Seven Years of Coronal Hole Observations With the SXT

GREGORY SLATER (LOCKHEED MARTIN SOLAR AND ASTROPHYSICS LABORATORY 1027 TANLAND DR. #110, PALO ALTO, CA 94303)

The Soft X-ray Telescope (SXT) aboard the Yohkoh satellite has imaged unipolar regions in the solar corona for seven years, through the transition from solar maximum to solar minimum and the onset of a new solar cycle. This work presents a summary of the observations, with particular attention to cyclic variations, including boundary evolution, coverage, and emission measure and temperature distributions. Comparisons are made with EIT and TRACE observations in the periods of overlap.

(71)

“Flat Fields” for UVCS Detectors

P. L. SMITH, R. SULEIMAN, L. D. GARDNER, M. COSMO, N. ATKINS & J. L. KOHL

Use of UVCS/SOHO requires knowledge of the absolute sensitivity for detecting photons at all wavelengths in its bandpass and everywhere in the field of view. One component of this is the pixel-to-pixel sensitivity of the detectors, i.e., the “flat field.”

Because UVCS has no provision for uniformly “flooding” its detectors with solar (or other) UV photons, a boot strap method had to be devised. The process is: (i), to observe a star to determine the flat field for one or more columns of pixels, and, then, (ii), to observe the spectrum of scattered disk light with a large number of closely spaced grating positions to determine the flat field of other columns relative to the first few.

We will discuss the methods used to determine the detector flat fields, certain complications, the results, and their limitations.

(72)

On the electron heat flux regulation in the solar wind through wave-particle interactions

J. SOLOMON, F. PIERRE (IAS/CNRS/UNIV. PARIS-XI, ORSAY, FRANCE), N. CORNILLEAU-WEHLIN, P. CANU (CETP/CNRS, VELIZY, FRANCE), E. E. SCIME (DEPT OF PHYSICS, WEST VIRGINIA UNIVERSITY, MORGANTOWN, WV, USA), A. BALOGH, R. FORSYTH (IMPERIAL COLLEGE OF SCIENCE AND TECHNOLOGY, LONDON, GB)

Magnetic whistler-mode wave spectra measured by the Ulysses'wave experiment (URAP; frequency range 0.22-448 Hz) correlate well with the wave growth rates of the electromagnetic electron cyclotron instability. These growth rates are computed from the electron distribution functions obtained from the Ulysses'plasma experiment (SWOOPS; energy range 1.6-862 eV). We examine whether the halo electron heat flux can be the source of the instability and whether the emitted waves can in turn regulate the halo and core electron heat fluxes.

(73)

A study of the coronal hole - streamer interface

D. SPADARO, R. VENTURA, M. ALICATA (OSSERVATORIO ASTROFISICO DI CATANIA, ITALY), S. FINESCHI, C. BENNA (OSSERVATORIO ASTRONOMICCO DI TORINO, ITALY), A. CIARAVELLA (UNIVERSITÀ DI PALERMO, ITALY), R. O'NEAL (SAO, CAMBRIDGE, MA), A. MODIGLIANI (UNIVERSITÀ DI FIRENZE, ITALY), R. SULEIMAN (SAO, CAMBRIDGE, MA), G. NOCI (UNIVERSITÀ DI FIRENZE, ITALY), AND J. L. KOHL (SAO, CAMBRIDGE, MA)

We investigate the behaviour of line intensities and profiles, measured by the UVCS/SOHO spectrocoronagraph, across the interface region between coronal holes and streamers. Our aim is to study whether there is a sharp difference in the profile width and intensity of the examined spectral lines, as well as in the O VI line intensity ratio, or the change of these parameters is smooth. The results can give some indications about the interactions between the coronal holes and the surrounding regions plasma.

(74)

Acceleration Profile Of the Slow Solar Wind as inferred from gradual mass ejections observed by LASCO

N. SRIVASTAVA, R. SCHWENN, B. INHESTER, G. STENBORG AND B. PODLIPNIK

The slow solar wind (< 400 km/s) appears to initiate from the regions in the corona, where magnetic fields are closed, or from the interface between streamers and other coronal regions. However, the nature of the acceleration profile of slow solar wind is not yet well known. LASCO observations of gradually evolving mass ejections which seem to trace out the slow solar wind, offer us a good opportunity to study the speed and acceleration profiles of the slow solar wind from a distance of 1.1 up to 30 solar radii. In this paper, we present the speed and acceleration profiles of slow solar wind, derived on the basis of measurements of mass flows in several cases of gradual mass ejections and present them in perspective of earlier works.

(75)

Recent observations of the solar corona with a new ground-based mirror coronagraph in Argentina (MICA)

G. STENBORG (1), RAINER SCHWENN (1), N. SRIVASTAVA (1), B. INHESTER (1), B. PODLIPNIK (1), M. ROVIRA (2) AND C. FRANCILO (3)

(1) MAX PLANCK INSTITUT FUER AERONOMIE, D 37191 KATLENBURG-LINDAU, GERMANY

(2) INSTITUTO DE ASTRONOMIA Y FISICA DEL ESPACIO (IAFE), C.C. 67 - SUC. 28, 1428 BUENOS AIRES, ARGENTINA

(3) OBSERVATORIO ASTRONOMICCO FELIX AGUILAR (AOFA), BENAVIDEZ 8175 OESTE, 5413 CHIMBAS, SAN JUAN, ARGENTINA

As part of the new German-Argentinian Solar-Observatory in El Leoncito, San Juan, Argentina, a new ground-based solar telescope (MICA: Mirror Coronagraph for Argentina) began to operate in August 1997. MICA is an advanced mirror coronagraph, its design being an almost exact copy of the LASCO-C1 instrument. Since its installation, it has been imaging the inner solar corona (1.05 to 2.0 solar radii) in two spectral ranges, corresponding to the emission lines of the

Fe XIV and Fe X ions. The instrument can image the corona as fast as every minute. Thus, it is ideally suited to study fast processes in the inner corona. In this way it is a good complement for the LASCO-C1 instrument. After a brief review of the characteristics of the instrument, we present some recent observations. We show the structural and temporal evolution of the inner corona and compare the observations with those obtained by LASCO.

(76)

Constraints on Coronal Outflow Velocities derived from UVCS Doppler Dimming Measurements and In-Situ Charge State Data

L. STRACHAN, Y.-K. KO, A. V. PANASYUK, D. DOBRZYCKA, J. L. KOHL (HARVARD-SMITHSONIAN CFA); M. ROMOLI, AND G. NOCI (UNIV. OF FLORENCE); S. E. GIBSON (NASA/GSFC); D. A. BIESECKER (NRL)

We constrain coronal outflow velocity solutions, resolved along the line-of-sight, by using Doppler dimming models of H I Lyman alpha and O VI 1032/1037 Angstrom emissivities obtained with data from the Ultraviolet Coronagraph Spectrometer (UVCS) on SOHO. The local emissivities, from heliocentric heights of 1.5 to 3.0 radii, were determined from 3-D reconstructions of line-of-sight intensities obtained during the first Whole Sun Month Campaign (10 Aug. to 8 Sep. 1996). The models use electron densities derived from polarized brightness measurements made with the visible light coronagraphs on UVCS and LASCO, supplemented with data from Mark III at NCAR/MLSO. Electron temperature profiles are derived from 'freezing-in' temperatures obtained from an analysis of charge state data from SWICS/ Ulysses. The work concentrates on neutral hydrogen outflow velocities which depend on modeling the absolute coronal emissivities. We use an iterative method to determine the neutral hydrogen outflow velocity with consistent values for the electron temperatures derived from a freezing-in model.

This work is supported in part by NASA under grant NAG-3192 to the Smithsonian Astrophysical Observatory, by the Italian Space Agency and by Swiss funding agencies.

(77)

Coronal Holes versus normal Quiet Sun observed with SUMER

K. STUCKI, S. K. SOLANKI, I. RUEDI, J. O. STENFLO, A. BRKOVIC (INSTITUTE OF ASTRONOMY, ETH, CH-8092 ZUERICH, SWITZERLAND)

U. SCHUEHLE, K. WILHELM (MAX-PLANCK-INSTITUT FUER AERONOMIE, MAX-PLANCK-STR. 2, D-37191 KATLENBURG-LINDAU, GERMANY)

M. C. E. HUBER (ESA, SPACE SCIENCE DEPARTMENT, ESTEC, NL-2200 AG NOORDWIJK, THE NETHERLANDS)

We analyse SUMER spectra of 15 lines of 11 ions, obtained on both sides of the boundary of polar coronal holes as well as at the equator during the SOHO roll manoeuvre of March 1997.

We compare line intensities, shifts, widths and asymmetries in coronal holes with values obtained in the quiet Sun.

We find that coronal lines show a blueshift in coronal holes relative to the quiet Sun, while there is no evidence for such a shift at ion temperatures below 10^5 K. The width of the lines is generally larger (by 10-20 km/s) inside the coronal hole, while intensity measurements show a great dispersion.

We refine this analysis for the lines Ne VIII (770.41 Angstroms) and Fe XII (1242.02 Angstroms) using further coronal hole data (JOP055), as well as additional lines formed at coronal temperatures (JOP055 CDS data).

(78)

Streamer evaporation

S. T. SUESS, A.-H. WANG, S. T. WU, S. F. NERNEY

Evaporation is the consequence of slow plasma heating near the tops of streamers where the plasma is only weakly contained by the magnetic field. The form it takes is the slow opening of field lines at the top of the streamer and transient formation of new solar wind. It was discovered in polytropic model calculations, where due to the absence of other energy loss mechanisms in magnetostatic streamers, its ultimate endpoint is the complete evaporation of the streamer. This takes, for plausible heating rates, weeks to months in these models.

Of course streamers do not behave this way, for more than one reason. One is that there are losses due to thermal conduction to the base of the streamer and radiation from the transition region. Another is that streamer heating must have a characteristic time constant and depend on the ambient physical conditions. We use our global MHD model with thermal conduction to examine a few examples of the effect of changing the heating scale height and of making ad hoc choices for how the heating depends on ambient conditions. At the same time, we apply and extend the analytic model of streamers developed by Pneuman (1968), which showed that streamers will be unable to contain plasma for temperatures near the cusp greater than $\sim 2 \times 10^6$ K.

Slow solar wind is observed to come from streamers through transient releases. A scenario for this that is consistent with the above physical process is that heating increases the near-cusp temperature until field lines there are forced open. The subsequent evacuation of the flux tubes by the newly forming slow wind decreases the temperature and heating until the flux tubes are able to reclose. Then, over a longer time scale, heating begins to again refill the flux tubes with plasma and increase the temperature until the cycle repeats itself. The calculations we report here are first steps towards quantitative evaluation of this scenario.

Pneuman, G. Some general properties of helmeted coronal structures, *Sol. Phys.*, v3, pp 578-597, 1968.

(79)

Ulysses-UVCS Coordinated Observations.

S. SUESS, G. POLETTI, G. SIMNETT

We present results from coordinated observations in which instruments on SOHO and Ulysses were used to measure the density and flow speed of plasma at the Sun and to again measure the same properties of essentially the same plasma in the solar wind. Plasma was sampled by UVCS at 3.5 and 4.5 solar radii and by Ulysses at 5 AU. Data were acquired during a nearly 2 week period in May-June 1997 at a latitude of 9-10 degrees north of the equator, on the east limb and, hence, in the streamer belt region and the source location of slow wind. Density and outflow plasma speed are compared, in order to check for preservation of the near Sun characteristics in the interplanetary medium. By chance, Ulysses was at the very northern edge of the visible streamer belt. Nevertheless, no evidence of fast wind, or mixing with fast wind coming from the northern polar coronal hole was evident at Ulysses. The morphology of the streamer belt was the same at the beginning and end of the observation period, but

changed markedly during the middle of the period. A corresponding change in density (but not flow speed) was noted at Ulysses.

(80)

UVCS/SOHO Observations of H I Lyman Alpha Line Profiles in Coronal Holes at Heliocentric Heights above $3.0 R_{\odot}$

R. M. SULEIMAN¹, J. L. KOHL¹, R. FRAZIN¹, A. CIARAVELLA^{1,2}, S. R. CRANMER¹, L. D. GARDNER¹, R. HAUCK¹, A. V. PANASYUK¹, P. L. SMITH¹ AND G. NOCI³

¹ HARVARD-SMITHSONIAN CENTER FOR ASTROPHYSICS, CAMBRIDGE, MASS., USA

² ESA SPACE SCIENCE DEPARTMENT, ESTEC, NOORDWIJK, THE NETHERLANDS

³ UNIVERSITÀ DI FIRENZE, FIRENZE, ITALY

The Ultraviolet Coronagraph Spectrometer (UVCS) aboard the SOHO spacecraft is designed to probe the solar corona from 1.25 to 10 R_{\odot} from sun center through the observation of ultraviolet spectral lines. In polar coronal holes, H I Lyman α is the most intense observable line with UVCS above 3.0 R_{\odot} . This is the region where the outflowing coronal plasma becomes nearly collisionless and the ionization balance is believed to be frozen. At these heights, the H^0 velocity distribution may not be representative of the proton distribution because the characteristic time for charge transfer between H^0 and protons becomes longer than that for the outflow through, for example, a density scale height. Hence, the H^0 velocity distribution may not be directly affected by transverse wave motion or wave damping. In this paper we present measurements of H I Lyman α line profiles in coronal holes from 3.5 to above 6.0 R_{\odot} .

This work is supported by the National Aeronautics and Space Administration under grant NAG5-3192 to the Smithsonian Astrophysical Observatory, by Agenzia Spaziale Italiana, and by Swiss funding agencies.

(81)

Ion temperatures as observed in the solar corona and obtained in a solar wind model

C.-Y. TU (DEPARTMENT OF GEOPHYSICS, PEKING UNIVERSITY, 100871 BEIJING, CHINA)

E. MARSCH, K. WILHELM, W. CURDT (MAX-PLANCK-INSTITUT FUER AERONOMIE, MAX-PLANCK-STR. 2, D-37191 KATLENBURG-LINDAU, GERMANY)

The temperatures of some highly ionized ions in the polar coronal hole are determined from the widths of EUV lines measured by the SUMER (Solar Ultraviolet Measurements of Emitted Radiation) instrument on SOHO (Solar and Heliospheric Observatory). Radiations from both light ions, such as Ne VII, Ne VIII, Mg VIII, Mg X, Si VII, Si VIII, and heavy ions, such as Fe X, Fe XI and Fe XII, are recorded from off-limb observations. After subtraction of the instrument contribution the intrinsic line widths can be determined. By considering reasonable non-thermal or turbulent broadening contributions to the measured line widths, the range of ion kinetic temperatures can be delimited. The ion thermal temperatures are found to increase with increasing mass-per-charge number (A/Z) of the ions for A/Z greater than a certain value, which seems to decrease from 4 to 3 between 1.05 and 1.15 solar radii. These trends are interpreted as evidence supporting the ion-cyclotron-resonance heating mechanism, whereby the energy is supplied by outward-propagating high-frequency Alfvén waves. Based on this mechanism, a

two-fluid model was developed. Some of the model results are presented. The consistency of our results with recent UVCS observations also favours the ion-cyclotron-resonance mechanism for the coronal heating.

(82)

UVCS observations of coronal streamers and theoretical models: structure and oxygen abundance

A. M. VÁSQUEZ (1,2), J. C. RAYMOND (1), AND A. VAN BALLEGOIJEN (1)

(1) SMITHSONIAN ASTROPHYSICAL OBSERVATORY, 60 GARDEN ST., CAMBRIDGE, MA 02138, U.S.A. EMAIL: AVASQUEZ@CFA.HARVARD.EDU

(2) GRADUATE STUDENT OF BUENOS AIRES UNIVERSITY, ARGENTINA

We present results derived from the analysis of equatorial streamer structures as observed by the UVCS instrument aboard SOHO. From the observed LOS integrated profiles and intensities of the H I Ly α and Ly β lines, we infer the density and temperature of the plasma through the streamer structure. From these estimates, as well as field extrapolations from Kitt Peak synoptic maps, we model the observed structures with the aid of a static MHD model. The inferred plasma β is clearly of order one in the closed field regions, and much higher near the cusps of the structures. Then, our model contains the effects of pressure gradients on the magnetic field lines.

Previous analysis of the O VI 1032/1037 lines (also observed by UVCS) shows a large depletion of oxygen and other high-FIP elements in the streamer's closed field regions. We show here results of analyzing these lines for the observed streamers. Using our inferred knowledge of their 3D structure, we determine projection effects on the observed intensities, and determine the oxygen abundances both in the open and closed field regions.

(83)

Alfven Waves from the Transition Region and “Solar Tornadoes”

M. VELLI, P. C. LIEWER AND D. KONDRASHOV (JPL)

We discuss the properties of Alfvén waves generated in the photosphere by vortex sinks and propagating upwards through the transition region and corona, and contrast them to Alfvén waves generated via reconnection in transition region “explosive events”. Though the propagation of Alfvén waves has been considered before, we focus here on the behaviour of a number of coherent sources turned on intermittently and their role in the overall solar wind dynamics above coronal holes. We also present preliminary numerical simulations in 2 and 3 dimensions and compare such large amplitude waves with the properties of rotating macro-spicules and the rotating transition region features observed by CDS on SOHO.

(84)

CDS/SOHO spectral variations in and around coronal holes

PETER YOUNG (DEPARTMENT OF APPLIED MATHEMATICS AND THEORETICAL PHYSICS, SILVER STREET, CAMBRIDGE CB3 9EW, UNITED KINGDOM)

Spectra obtained from a variety of solar structures by the Coronal Diagnostic Spectrometer (CDS) on board SOHO are compared. In particular, coronal holes are studied and spectral variations both within a coronal hole and across a coronal hole boundary are discussed.

The ability of CDS to fully separate spatial and spectral dimensions ensures that different regions can be readily isolated, while the broad range of both temperature and density diagnostics allow small differences in plasma conditions to be identified.

(85)

Latitudinal properties of the Ly α and O VI profiles in the extended solar corona

L. ZANGRILLI, P. NICOLOSI, G. POLETTO

We have analyzed the latitudinal properties of the line profiles of H I Lyman alpha line and O VI doublet at 1032 Å and 1037 Å in the extended solar corona, between $1.5 R_{\odot}$ and $1.8 R_{\odot}$. Observations have been performed with the UltraViolet Coronagraph Spectrometer (UVCS) on board the ESA-NASA solar satellite SOHO (Solar and Heliospheric Observatory). The results show that these lines have a quite different behaviour with latitude: the Lyman alpha line presents larger FWHM values in the streamer region and narrower ones towards the polar latitudes, while the O VI lines present a minimum FWHM at the center of the streamer and an almost steady increase towards the polar region. The observations have been analyzed looking also for possible correlations with the intensity of the coronal lines. Plausible interpretation in terms selective heating mechanisms are discussed.

(86)

Radial variation of the coronal helmet streamer belt

X. P. ZHAO AND J. T. HOEKSEMA

Coronal and heliospheric observations made by SOHO and Ulysses provide an opportunity to determine the radial variation of the coronal helmet streamer belt near sunspot minimum. The radial variation of the belt's thickness is affected by the radial variation of nearby coronal hole boundaries. This also applies to the heliospheric current sheet, which is the radial extension of the streamer belt. Using the radial variation of the coronal helmet-streamer belt observed by SOHO and the northward extension of the heliospheric current sheet observed by Ulysses, we can optimize the free parameters in the current-sheet source-surface model applied to MDI photospheric data. This allows determination of the radial variations of the coronal open field regions and the neutral line from near solar surface to 1 AU.

(87)

Elemental abundances in different solar regions

F. ZUCCARELLO (INSTITUTE OF ASTRONOMY, VIALE A. DORIA 6, CATANIA, ITALY)

Many authors have indicated that the elemental abundances measured in the outer solar atmosphere might differ from those measured in the photosphere, and that abundances variations within the transition region and the corona, among features characterized by different magnetic topologies and physical conditions, may occur. However, there is not general agreement at present on the existence of such abundance variations and on the mechanisms for producing

them. On the other hand, spacecraft measurements have shown that the abundances in the solar wind show temporal variations in the chemical composition, and this variability could reflect differences in the chemical composition among different source regions. In this context, we have analyzed EUV spectra in order to search for empirical evidences in the corona explaining the variability of the solar wind and to study the dependence of the chemical composition on the type of coronal structure.

(88)

The Transition from Fast and Slow Solar Wind: Experimental Constraints on Solar Wind Theories

T. H. ZURBUCHEN, S. HEFTI, L. A. FISK, G. GLOECKLER, N. A. SCHWADRON, R. VON STEIGER

It is generally believed that fast solar wind originates in coronal holes and expands to low latitude. Slow solar wind, however, originates from closed magnetic field regions. This simple model has been repeatedly challenged based on both solar and heliospheric observations. For example, it has been proposed that the solar wind could expand more radially from all solar latitudes.

Since many of the dynamic parameters of the solar wind are changed during its expansion through the heliosphere, it is hard to test those theories *in situ*. However, using charge state and elemental composition data as measured with Ulysses-SWICS and ACE-SWICS, we are able to get a very detailed view of various solar wind streams which are not affected by processes occurring away from the sun.

We will present Ulysses-SWICS and ACE-SWICS data which indicate that the fast and slow solar wind are fundamentally different. It will be shown that the transition from one regime into the other is very abrupt and occurs on the shortest time-resolution of the sensors. We will present new data and discuss them in the framework of the theories mentioned above.

(89)

Physical and Dynamical Parameters of a CME observed with SOHO

A. CIARAVELLA^{1,2}, J. RAYMOND¹, B. THOMPSON³, J. LI¹, R. O'NEAL¹, J. KOHL¹, G. NOCI⁴

¹ HARVARD-SMITHSONIAN CENTER FOR ASTROPHYSICS

² DIPARTIMENTO DI SCIENZE FISICHE & ASTRONOMICHE, PALERMO, ITALY

³ SPACE APPLICATIONS CORPORATION, VIENNA VA

⁴ UNIVERSITY OF FLORENCE, ITALY

In two years of observations many Coronal Mass Ejection (CME) have been observed with the Ultraviolet Coronagraph Spectrometer (UVCS) aboard SOHO, and spectroscopic diagnostics of these events is now available. In this poster we present an event observed on Dec 12, 1997 with LASCO C1 and C2, EIT, UVCS. A morphological description of the event as detected in the several spectral band is described along with the spectroscopic analysis of physical and dynamical proprieties of the ejected plasma. In the UVCS spectra cooler lines, as C III (977.02 Å), Si III (1206.51 Å), N V (1242.80 and 1238.82 Å), Ly α , Ly γ , OVI (1031.91 and 1037.61 Å) shown very large excursions while no signs is detected in the high temperature lines as Si XII (520.66 and 499.37 Å), [Fe XII] (1242.00 Å) and [S X] (1196.24 Å). The UVCS spectra show the same helical motion seen in the LASCO C2 images. Very large Doppler shifts were observed

and the line of sight velocities for the different ejected component are determined. Velocity up to 200 km/sec have been detected. The Doppler Dimming analysis of the O VI lines gives constraint on the outflow velocities of the the ejected material.

(90)

Enhanced abundance of oxygen and iron in polar coronal holes, from CDS, SUMER and LASCO data

A. H. GABRIEL, F. BELY-DUBAU, C. DAVID, P.LAMY AND E. QUEMERAIS

The abundance of oxygen and iron relative to that of free electrons is compared between a polar coronal hole and an equatorial closed-field region, over the range 1.05 to 1.3 R_{\odot} . The oxygen and iron data are obtained from the CDS and SUMER sequences recorded during the solar minimum for the JOP2 observations, aimed at electron temperature measurements (David et al, A&A, in press). For the ratio of electron density between the two regions, we have adopted typical values, as determined frequently from eclipse observations. These have been compared with values obtained from LASCO C2 above 2 R_{\odot} at the same time as the spectroscopic data, and extrapolated to lower heights. We find substantial enhancements of the order $\times 10$ in the abundance of oxygen and iron in coronal hole regions. Such enhancement of heavy elements with respect to hydrogen has implications for the initial acceleration of the solar wind and for the understanding of wind abundances observed near 1 A.U.

INDEX OF AUTHORS

Aletti, V 28	Costa, J 11	Gloeckler, G 20, 24, 45
Alicata, M 39	Cranmer, S R 14, 26, 42	Goedbloed, J P 26
Altrock, R C 10	Curdt, W 37, 42	Goldstein, B E 29
Andretta, V 25	Cuseri, I 14	Gombosi, T I 21
Antonucci, E 10, 20	Dahlburg, R B 15	Groth, C P T 21, 26
Atkins, N 38	Dammasch, I E 15, 23	Guhathakurta, M 17, 21, 31
Axford, W I 10	David, C 46	Hackenberg, P 22
Balogh, A 38	Davila, J M 16	Hakamada, K 27
Bely-Dubau, F 46	DeForest, C 32	Hansteen, V H 22
Benna, C 39	Del Zanna, G 16	Harvey, K L 23
Bertaux, J-L 11	Dennis, E 19	Hassler, D M 23, 28
Betta, R 12	Deshpande, M R 33	Hathaway, D H 18
Biesecker, D A 40	De Zeeuw, D L 21	Hauck, R 42
Bocchialini, K 28	Dobrzycka, D 17, 17, 40	Hearn, A G 30
Bochsler, P 24	Dodero, M A 10	Hefti, S 20, 24, 45
Bodmer, R 12	Einaudi, G 15	Hoeksema, J T 44
Boncinelli, P 15	Esser, R 26	Hood, A 23
Bout, M 27	Falconer, D A 18, 32, 36	Hovestadt, D 19
Brkovic, A 40	Field, G B 14	Howard, R A 23, 32
Bromage, B J I 12, 14, 16	Fineschi, S 18, 19, 26, 39	Huber, M C E 40
Browning, P K 14	Fisher, R 17, 31	Inhester, B 37, 39, 39
Brueckner, G E 25	Fisk, L A 18, 20, 24, 45	Insley, J 24
Burlaga, L F 13	Fludra, A 13, 19	Ipavich, F M 19, 20, 24
Canu, P 38	Forsyth, R 38	Jones, H P 25
Chae, J 35	Francile, C 39	Kallenbach, R 19, 24
Chiuderi, C 13	Frazin, R A 19, 42	Karovska, M 25
Chiuderi Drago, F 13	Gabriel, A H 46	Karpen, J T 15
Ciaravella, A 19, 26, 39, 42, 45	Galvin, A B 19	Keppens, R 26
Clegg, J R 12, 14	Gardner, L D 17, 19, 26, 31, 38, 42	Kerdraon, A 13
Cook, J W 25	Geiss, J 20	Ko, Y-K 26, 40
Cornilleau-Wehrlin, N 38	Gibson, S E 20, 40	Kohl, J L 14, 17, 17, 18, 19, 26, 31, 32, 38, 39, 40, 42, 45
Cosmo, M 38	Giordano, S 10, 20	

Kojima, M	27	Olsen, E L	33	Shah, K J	33
Kondrashov, D	43	Om Vats, H	33	Simnett, G	41
Koomen, M J	31	O'Neal, R	19, 39, 45	Sittler, E, Jr	21
Kyrola, E	11	Orlando, S	12	Slater, G	38
Lallement, R	11	Panasyuk, A V	17, 40, 42	Solanki, S K	37, 40
Lamy, P	27, 46	Paquette, J A	19, 24	Solomon, J	38
Landi, E	13, 27, 28	Paswaters, S	31	Smith, P L	17, 31, 38, 42
Landini, M	28	Patsourakos, S	34	Spadaro, D	39
Leer, E	33	Penn, M J	25	Srivastava, N	37, 39, 39
Lemaire, P	23, 28	Peres, G	12	St. Cyr, C	32
Li, J	45	Pierre, F	38	Stenborg, G	37, 39, 39
Li, X	28	Pisanko, Y V	34	Stenflo, J O	40
Liewer, P C	29, 43	Plunkett, S P	31	Stout, Q F	21
Llebaria, A	27	Podlipnik, B	37, 39, 39	Strachan, L	17, 17, 18, 31, 40
Maccari, L	29	Poedts, S	34	Stucki, K	37, 40
Mahajan, S M	34	Poland, A I	35	Suess, S T	32, 41, 41
Makinen, T	11	Poletto, G	14, 32, 41, 44	Suleiman, R	26, 38, 39, 42
Mann, G	22	Porter, J G	18, 32, 36	Summanen, T	11
Marsch, E	22, 30, 42	Powell, K G	21	Thompson, B	12, 45
Marshall, H G	21	Quemerais, E	11, 27, 46	Tokumar, M	27
Martens, P C H	30	Raymond, J C	19, 36, 43, 45	Tu, C-Y	42
Mehta, M	33	Recely, F	23	Tziotziou, K	30
McKenzie, J F	10	Rogava, A	34	van Ballegooijen, A	43
Michels, D J	31	Romashets, E	36	Vasquez, A M	43
Michels, J	19	Romoli, M	18, 32, 37, 40	Velli, M	29, 43
Miralles, M P	17, 31	Rovira, M	39	Ventura, R	39
Modigliani, A	19, 26, 39	Ruedi, I	40	von Steiger, R	45
Moore, R L	18, 32, 36	Schmidt, W	11	Wang, A-H	41
Mullan, D J	14	Schuehle, U	37, 40	Wang, A-W	31
Nerney, S F	41	Schwadron, N A	45	Warren, H	23
Nicolosi, P	44	Schwenn, R	37, 39, 39	Wilhelm, K	12, 23, 28, 37, 40, 42
Noci, G	14, 18, 19, 26, 32, 39, 40, 42, 45	Scime, E E	38	Wimmer-Schweinbruber, R F	24
Ofman, L	16, 32	Serio, S	12	Wood, B	25
Ohmi, T	27	Shah, C R	33	Wu, S T	31, 41

Wurz, P	19	Zangrilli, L	44	Zurbuchen, T H	20, 24, 45
Yokobe, A	27	Zhao, X P	44		
Young, P	43	Zuccarello, F	44		